Effect of Reversed Loading on Shear Behavior of Reinforced Concrete

Thammanoon Denpongpan

A Dissertation submitted to
Kochi University of Technology
In partial fulfillment of the requirements for
the Degree of Master of Engineering

January 2001

ABSTRACT

During Hyogoken-Nanbu Earthquake in 1995, severe damages were encountered in many RC structures including RC column of bridge piers, which support highway and railway. Observations showed that shear failures with diagonal shear crack were prominent among those damages. During earthquake occurring, earthquake wave will produce force in any direction. Hence reversed loading is appropriate to assimilate this condition. Therefore shear behavior of RC short beam under reversed loading is necessary to investigate. RC deep beam is particular RC structures, which are usually found in transfer girders used in multistory buildings to provide column offsets, in foundation walls, and shear wall. In contrast to an ordinary beam, the depth of beam is comparable to its span length. RC short beam with a/d 1.5 have been selected in this study. To clarify shear mechanism in concrete solely, RC short beams without web reinforcement were studied at first place.

The experimental frameworks were divided into two series according to percentage of main reinforcement, 1.15 or 1.805%. Nine RC beam without web reinforcement were tested in this investigation. All beams were doubly reinforced with equaling tension and compression steel in each case. The variables were reinforcement ratio, 1.15 or 1.805%, and loading pattern, monotonic or reversed loading. Deform bars having yield strength 364 N/mm^2 for diameter 13-mm. and 336 N/mm^2 for diameter 16-mm. were used as flexural reinforcement. Ordinary Portland cement with limestone 40% replacement, sea sand, crush sand, aggregate and superplasticizer were used. Same mix proportion of self-compacting concrete (SCC) with medium strength between 52-58 N/mm^2 was used in this experiment. In the area where you cannot easily reach, SCC with medium to high strength is appropriate to use in real application. Twelve 150x200 mm. cylinders were cast to determine the concrete compressive strength including checking the concrete compressive strength whether reaches target strength and tensile strength. All beam and cylinder specimens were cast and cured in similar conditions. The beam and specimens were kept covered under polyethylene sheets until it reaches target strength and taken out 24 hours.

The test beams were simply supported and were subjected to mid-span one-point load. To obtain consistency of experimental results, two specimens were subject to the same load pattern for each series. Electrical strain gauges were placed at mid-span to measure strain in tension steel. Linear Variable Displacement Transducers (LVDT) was placed at all supports and mid-span point both sides for measuring support settlement due to bearing paste settlement, and mid-span deflection. Hence relative mid-span deflection can be calculated. The load was applied by 1000 KN universal testing machine. Test program was divided into monotonic and reversed loading. For revered loadings, the test beams were over turned upside down manually. From the test, it can be realized that experimental set-up was important to control the precision especially position of mid-span load. The load-unload paths were applied according to following stages: flexural

crack, diagonal shear crack, and first yield of tension steel. After this first yield, control displacement was applied.

The experimental results showed that RC beams without web reinforcement with low a/d could sustain the load greatly even forming of diagonal shear crack. This enhances capacity resulted from arch action, which transfers shear force directly through diagonal shear strut. The available strength from arch action is largely dependent on whether the resulting diagonal compression stress can be accommodated. The horizontal compressive force in concrete and the tension in the main reinforcement have to equilibrate the load. The behavior of diagonal shear crack can explain as; at once diagonal crack formed and spread toward the compression zone, this crack will penetrate and stop at the compression face, hence no sudden collapse occurs. Until the load is greatly higher than that the diagonal crack first form, failure by crushing of diagonal compressive strut or bond slip of tension steel will become.

Reversed loading gives identical yield load as same as monotonic but significantly lower ultimate deflection. To compare this ultimate deflection, ductility, which expresses the element capacity to undergo inelastic behavior and absorb energy, is appropriate to use. Several forms of ductility are available. In this study, displacement ductility was investigated. Displacement ductility is defined as the ratio of deflection at ultimate load to the deflection at first yield of the tension steel. Ultimate load is the maximum load applied for a beam during the test. For monotonic loading, higher reinforcement ratio, 1.805%, is higher displacement ductility compared to that of lower one, 1.15%. For reversed loading of reinforcement ratio 1.15%, displacement ductility decrease approximately 40% while that of reinforcement ratio 1.805%, displacement ductility decrease more than 50%. Hence higher reinforcement ratios will be higher loss of displacement ductility under reversed loading.

Finite element program namely WCOMD, which had been developed in the University of Tokyo, was used in this analysis. Effective RC zone, which is related to the bond characteristic of reinforcing bar, had been implemented. FE analysis show good agreement of yield load but slightly lower ultimate load than experimental one.

In conclusion, RC short beam without web reinforcement can carry load even forming of diagonal shear crack due to arch action, which transfer load directly to support through diagonal compressive strut. Effect of reversed loading reduces significantly displacement ductility after yield of tension steel approximately 40% for reinforcement ratio between 1.15-1.805% with shear span to depth ratio 1.5. Further study should be extended to normal concrete with compressive strength 30-35 N/mm^2. Since shear span to effective depth ratio of 1.0-2.5 is widely used, further study should be covering this range. Finally to approach real application, RC with web reinforcement should be exist. Low reinforcement ratio is selected to study at first place.

ACKNOWLEDGEMENTS

I would like to express my profound gratitude and deepest indebtedness to my advisor Professor Hiroshi SHIMA for his valuable advise, constructive suggestions, tireless guidance, and enduring patience throughout this study. Without him, I do not have a chance to continue study in Japan. I would like to express my deepest gratitude to Professor Hajime OKAMURA for his sharp suggestion, valuable guidance and kindness through out this research work.

Sincere word of gratitude must also go to the Professor Mikio KADOTA, co-advisor, and Professor Eijin OTANI, member of committee, for their valuable suggestion and comments.

I would like to express my profound gratitude to Assistant Professor Masahiro OUCHI for his kindness and constant support.

I would like to express my deepest indebtedness to Mr. Masaru UENO for his keen technical support, valuable advice, health look after, and enduring patient through out experimental works. Without him, very special technical problems cannot restore.

Sincere words of thank also go to Mr. Supakit Swatekititham and Ms. Krittiya Kaewmanee for their help in early stage of experimental work. My deepest and most sincere thanks are due to Mr. Songkram Piyamahant and Mr. Krit Kangvanpanich for their constant help throughout the crucial experimental work.

I would like to express my deepest appreciate to Mr. JUNG Jong-Hyuck and Mr. KIM Hee-Jin for permanent encouraging me to keep study in Japan and endless moral support, which absolutely contributed me to complete this dissertation and my life in Japan.

I, also, wish to thank Mr. Shigehisa Komatsu for his certainly help in all Japanese documents and kindness in any request.

I would like to express my deepest gratitude to Ms. Kubo MARIKO, Japanese teacher, for her truly kindness throughout the Japanese course and extra Japanese custom.

I would like to express my sincere words of thank to Mr. Chayanon Hansapinyo, doctoral student at Sirindhorn International Institute of Technology, Thailand, for his constant support in any request.

Finally, I would like to express my deepest appreciation to my parent and brother for their endless love and moral support that made me can endure and passed over the all obstacles.

CONTENTS

CHAPTER 1

INTRODUCTION

1.1 General

During Hyogoken-Nanbu Earthquake in 1995, severe damages were experienced in many RC structures including RC column of bridge piers, which support highway and railway. Observation shown that shear failure with diagonal shear crack were prominent among those of them.

RC deep beam is particular RC structures, which usually found in transfer girders used in multistory building to provide column offsets (Fig. 1-1), in foundation walls, and shear wall. In contrast to an ordinary beam, the depth of beam is comparable to its span length. The beam with shear span-to-depth ratio, a/d, less than 1.0 is classified as deep beam, and a beam with a/d exceeding 2.5 as ordinary beams. The beam between these two ranges is classified as short beam. RC short beam with a/d 1.5 have been selected in this study.

During earthquake occurring, earthquake force will introduce force unsystematically. Hence reversed loading is appropriate to assimilate this condition. Therefore shear behavior of RC short beam under reversed loading is necessary to investigate.

Fig. 1-1 Transfer girder [1].

1.2 Objectives and Scope of Study

The main objective of this research is to investigate effect of reversed loading on shear failure behavior. To clarify shear mechanism in concrete solely, RC short beams without web reinforcement were study at first place.

CHAPTER 2

LITERATURE REVIEW

2.1 Source of Shear Transfer

The transmission of shear force in concrete is mainly in the form of

- Shear stress of concrete in compression zone, V_c. (Fig. 2-1)
- Aggregate interlock across diagonal crack plan, V_a. Aggregate interlock is directly related to material properties of concrete i.e. maximum aggregate size, shape of aggregate, and tensile strength of concrete. A shear force can transfer via the bearing and overriding until crack width is large certainly.
- Dowel action of longitudinal, V_d. Dowel action is mainly related to detailing of reinforcement. In RC member, dowel action becomes active when cracking is major important; this stage is often reached in the ultimate load situation.
- Shear reinforcement, V_s.
- Arch action.

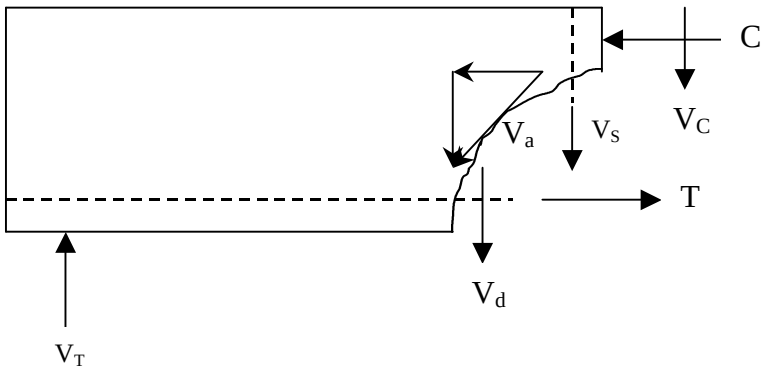

Fig. 2-1 Component of Shear force over crack plain.

From Fig. 2-1, the static equilibrium can express as follow

$$V_T = V_C + V_{av} + V_d + V_s$$

2.2 Beam Action and Arch Action

From Fig.2-2, the equilibrium of the section of beam between two crack can be written as

$$M = T \cdot jd$$

The relationship between shear and steel force can be written as

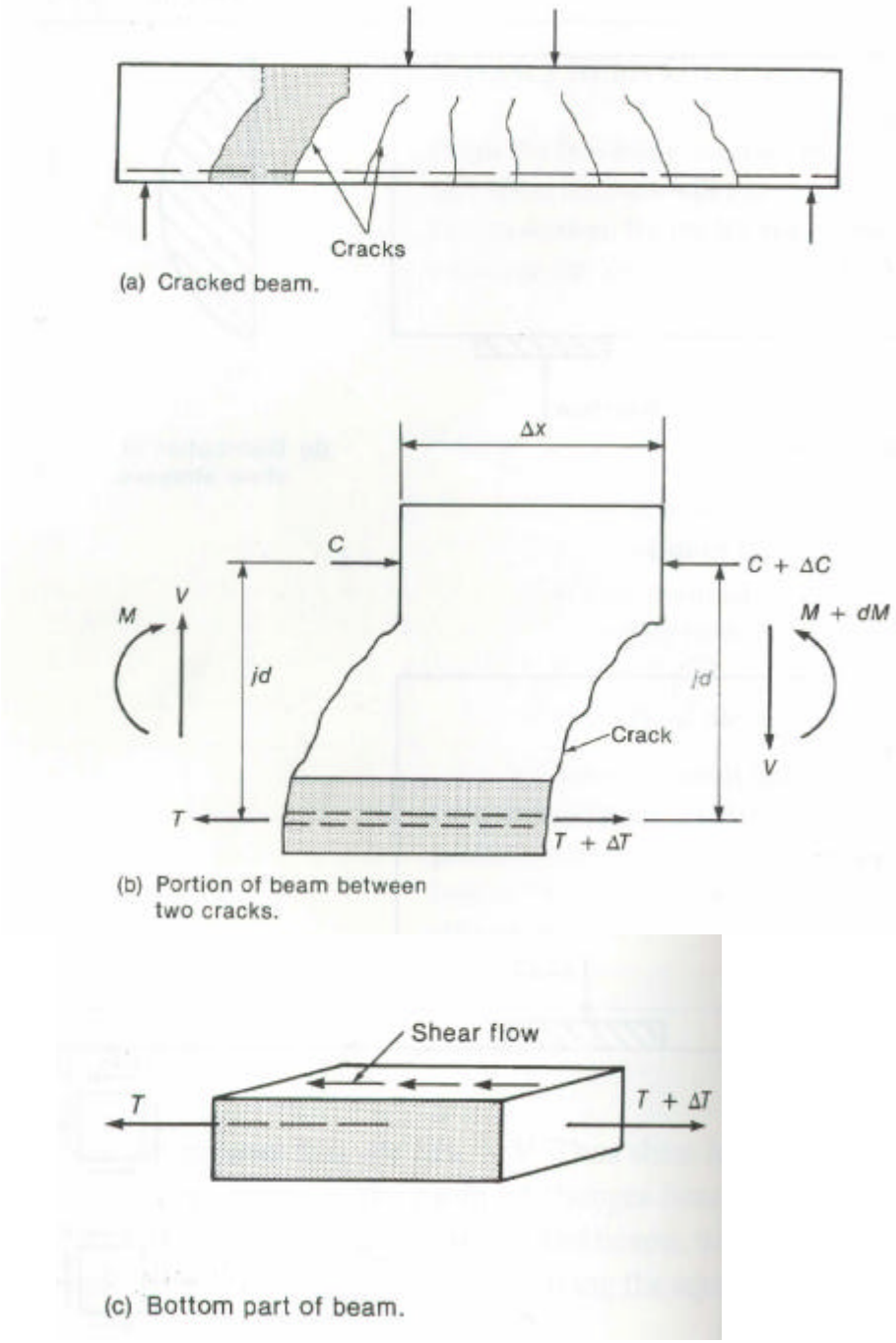

Fig. 2-2 Shear stress between cracks [1]

$$V = \frac{d}{dx}(T \cdot jd)$$

$$V = \frac{d(T)}{dx} jd + \frac{d(jd)}{dx} T$$

If the lever arms, jd, remains constant as assume in elastic beam theory,

$$\frac{d(jd)}{dx} = 0 \quad then \qquad V = \frac{d(T)}{dx} jd$$

where d(T)/dx is the shear flow across any horizontal plan between the reinforcement and the compression zone. This shear transfer mechanism is referred to *beam action*, which represent by shear flow over cross section.

On the contrary, if shear flow equal zero

$$\frac{d(T)}{dx} = 0 \qquad then \qquad V = T\frac{d(jd)}{dx}$$

This can occur if shear flow cannot be transmitted due to slip in main bar, or if the transfer of show flow is prevent by an inclined crack extending from the applied point load to support reaction. This shear transfer mechanism is referred to *arch action* (Fig. 2-3).

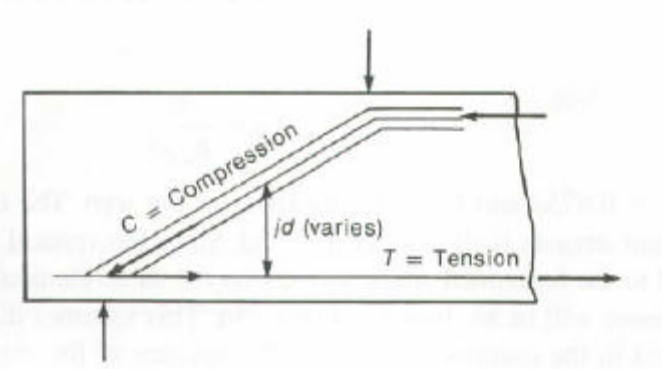

Fig.2-3 Arch action in a beam [1]

2.3 Behavior of Deep Beam Without Web Reinforcement

The available strength from arch action is largely dependent on whether the resulting diagonal compression stress can be accommodated. Short shear span, a/d from 1 to 2.5 develop inclined cracks, which able to carry the additional load by compressive strut (Fig.2-4). A significant part of the load is transferred directly from the point of applied load to the support by this diagonal compressive strut. The horizontal compression in concrete and the tension in the main reinforcement have to equilibrate the load. The geometry of this mechanism, which contributes shear strength, is clearly depending on placement of the loads and reactions. Failures usually due to crushing or splitting in diagonal compressive strut, which is close relationship to a splitting test of concrete cylinder.

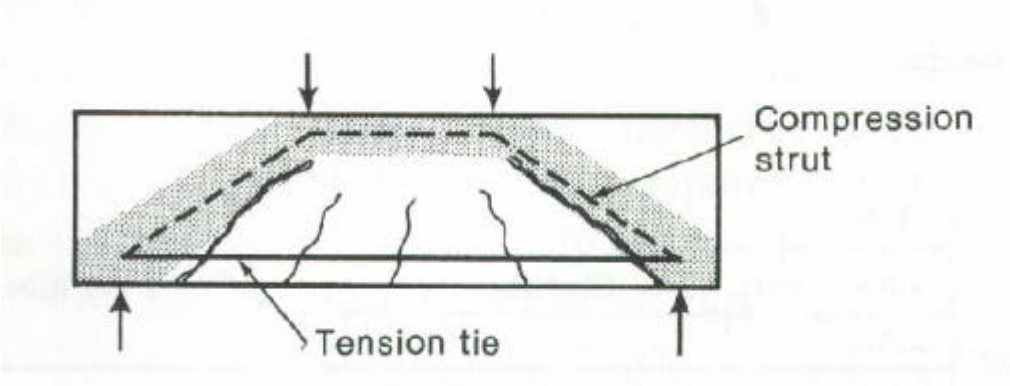

Fig. 2-4 Strut and tile model [1]

CHAPTER 3

EXPERIMENTAL PROGRAM

3.1 Test Specimens

The experimental frameworks are divided into two series according to percentage of main reinforcement, 1.15 or 1.805%. Nine RC beam without web reinforcement were test in this investigation. Fig.3-1 show beam dimensions, reinforcement details and loading arrangement for the beams. The test beams were simply supported and were subjected to mid-span one-point load. To obtain consistency of experimental results, two specimens were subject to the same load pattern for each series. Electrical strain gauges were instrumented at mid-span to measure strain in tension steel. Linear Variable Displacement Transducers (LVDT) was instrumented at all supports and mid-span point both side for measuring support settlement due to bearing paste settlement, and mid-span deflection. Hence relative mid-span deflection can be calculated. The load was applied by 1000 KN universal testing machine. All beams were doubly reinforced with equaling tension and compression steel in each case. The variables were reinforcement ratio and loading pattern, monotonic or reversed loading.

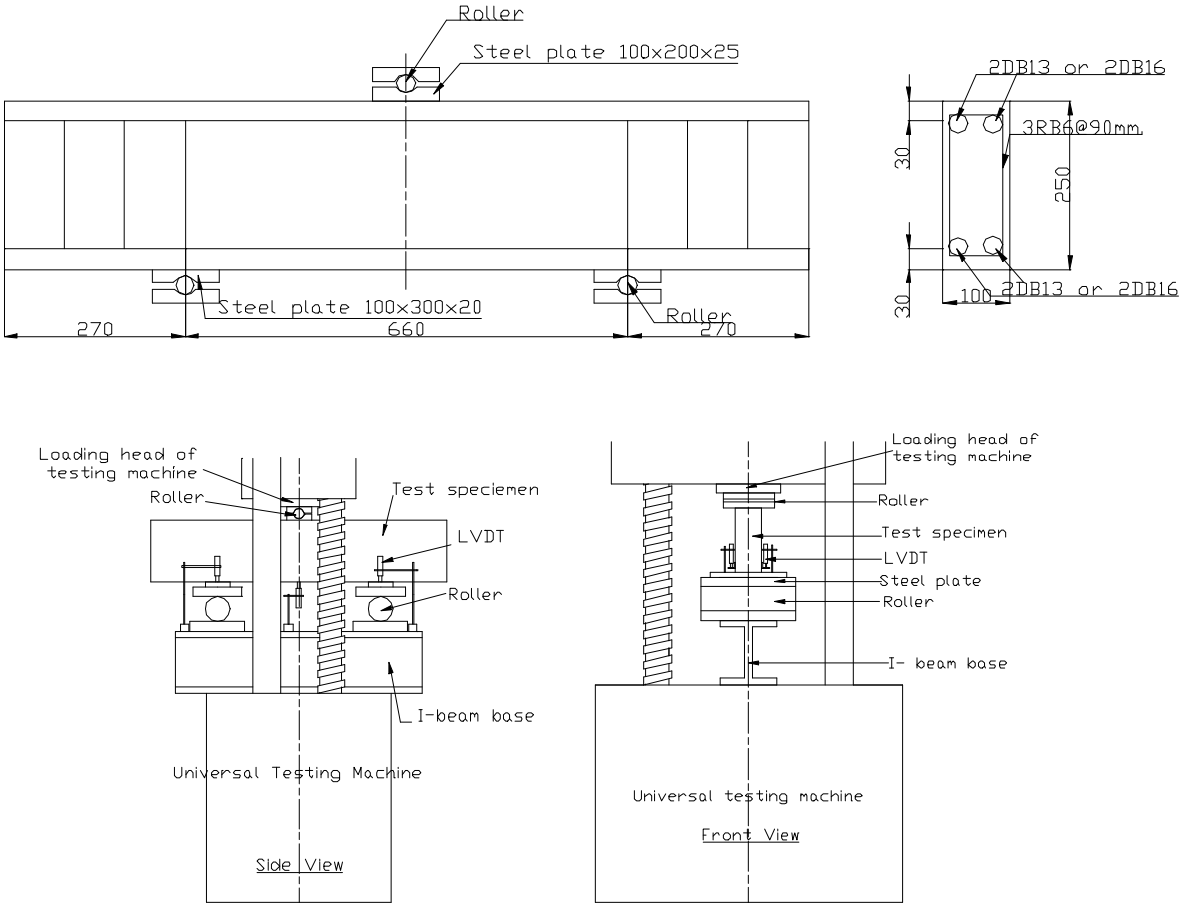

Fig. 3-1 Detail of test beam and testing arrangements (all dimension in mm.)

3.2 Material Properties

Ordinary Portland cement with limestone 40% replacement, sea sand, crush sand, aggregate and superplasticizer were used. Same mix proportion of self-compacting concrete (SCC) with medium strength between 52-58 N/mm^2 was used in this experiment. In hard-to- reach area, SCC couple with medium to high strength is appropriate to use in real application. Twelve 150x200 mm. cylinders were cast to determine the concrete compressive strength including checking the concrete compressive strength whether reaches target strength and splitting test. All beam and cylinder specimens were cast and cured similar conditions. The beam and specimens were kept covered under polyethylene sheets until 24 hours before testing. All materials properties are shown in Table 3-1.

Table 3-1Material Properties of concrete ingredient

	Specific Gravity	Absorption (%)
Ordinary Portland Cement	3.15	-
Lime Stone Powder	2.7	-
Small aggregate	2.69	-
Large aggregate	2.69	-
Sea Sand	2.57	1.91
Crush Sand	2.55	1.70

A rational mix-design method for self-compacting concrete was proposed by *Okamura* et. al in 1993 (Fig. 3-2) [8]. In this concept, concrete is assumed to be a two-phase material between coarse aggregate and mortar. Coarse and fine aggregate contents were proposed to limit at 50% of the solid volume in concrete and sand content were proposed to limit at 40% of mortar volume. At the given aggregate content level, optimum superplastizer to powder content ratio, Sp/P, and optimum water to cement ratio by volume, Vw/Vp will evaluated by trial and error technique.

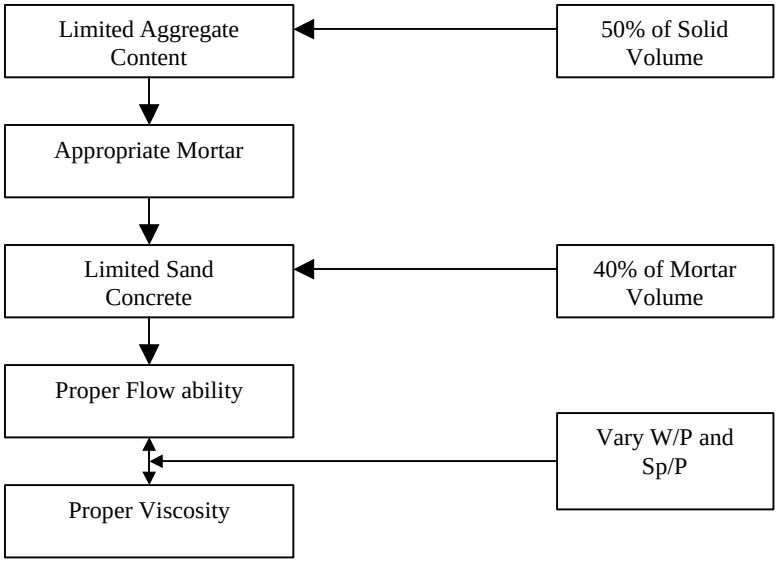

Fig. 3-2 Outline of a rational mix-design method for self-compacting concrete

The concrete mix proportion for all specimens are shown in Table 3-2.

Table 3-2 Concrete Mix Proportion

Ordnary portland cement with 40% limestone replacment

w/c	0.504	%
w/p (volume)	0.95	%
Water	184	kg/m^3
Ordinary Portland Cement	365	kg/m^3
Limestone Powder	201	kg/m^3
Sea Sand	386.48	kg/m^3
Crush Sand	389.52	kg/m^3
Small Gravel	592.7	kg/m^3
Large Gravel	253.8	kg/m^3
Superplasticizer	4.924	kg/m^3
Air Content	1.6	%

Note:

Sea Sand : Crush Sand (by volume)	50 : 50
Small Aggregate : Large Aggregate (by weight)	30 : 70
Superplasticizer	0.87% by weight of powder content
W_1	70% by volume of powder content

Deform bar having yield strength 364 N/mm^2 for diameter 13-mm. and 336 N/mm^2 for diameter 16-mm. were used as flexural reinforcement as shown by tensile test in Fig. 3-3 and Table 3-3.

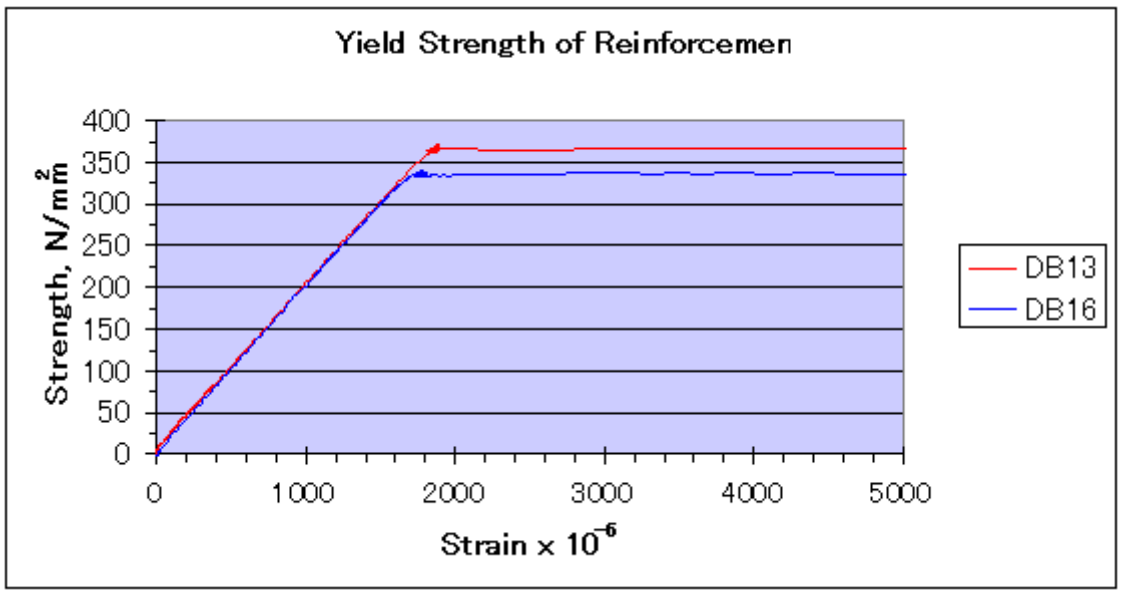

Fig. 3-3 Tensile test of reinforcement

Table 3-3 Properties of reinforcement

No.	Grade	Diameter mm	Cross Sectional Area mm^2	Yield Strength N/mm^2	Young Modulus N/mm^2
DB13	SD 295 A	12.7	126.7	364	203800
DB16	SD 295 A	15.9	198.6	336	203800

3.3 Mixing Method

Mixing order of all specimens are shown in Fig.3-4

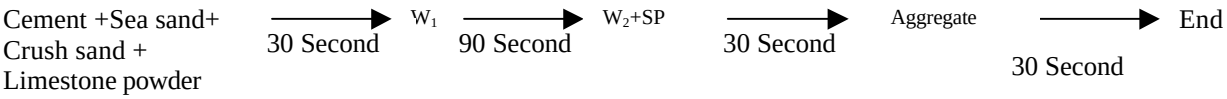

Fig. 3-4 Mixing method of SCC

3.4 Fresh Properties and Mechanical Properties

To ensure deformability and flow ability of self-compacting concrete, three standard self-compacting tests had been implement. First, flow ability of fresh concrete can measure by slump flow test; the optimum value (from test) is 650mm x 650mm. Second, filling ability can measure by U-type box test; minimum requirement is 300 mm. Last, concrete segregation can measure by V-funnel test; the minimum requirement is 10 sec. All concrete fresh properties are shown in Table 3-4.

Table 3-4 Properteis of Fresh Concrete

Beam Number	Slump flow mmxmm	Filling Height mm	Funnel Time sec	Concrete Temperature C^o
S1-1M	613 x 619	300	8.80	29.6
S1-2M	681 x 687	317	11.86	15.6
S1-3M	600 x 611	314	13.75	14.1
S1-4R	688 x 689	296	12.09	15.9
S1-5R	662 x 632	313	10.72	15.0
S2-1M	631 x 614	317	9.55	25.0
S2-2M	530 x 539	302	13.60	14.4
S2-3R	581 x 567	301	13.56	15.8
S2-4R	625 x 638	313	13.42	14.1

For mechanical properties of concrete, six standard cylindrical specimens of each test beam were used in compressive test. The maximum and minimum compressive strength of concrete were cut off, and the rest were used to determine average value. Four standard cylindrical specimens of each test beam also were used to determine tensile strength of concrete by splitting test. It can realize that precise set-up for splitting test is very important to obtained reliable data.

The empirical formula of tensile strength of concrete is used to compare with experimental one.

$$f_t = 0.23 f_C`^{\frac{2}{3}} \quad , f_C`(N/mm^2)$$

Testing program and mechanical properties of the tested beams are shown in Table 3-5.

Table 3-5 Testing program and mechanical properties of the tested beams

Beam Number	Load Pattern	$f_c`$ N/mm^2	f_{sp} N/mm^2	Diam. mm.	A_s mm^2	ρ (%)
S1-1M	Monotonic	52.2	-	2ϕ13	253.4	1.15
S1-2M	Monotonic	52.73	3.08	2ϕ13	253.4	1.15
S1-3M	Monotonic	57.18	2.8	2ϕ13	253.4	1.15
S1-4R	Reversed Cyclic	55.62	3.78	2ϕ13	253.4	1.15
S1-5R	Reversed Cyclic	56.57	3.41	2ϕ13	253.4	1.15
S2-1M	Monotonic	51.64	-	2ϕ16	397.2	1.805
S2-2M	Monotonic	55.32	3.2	2ϕ16	397.2	1.805
S2-3R	Reversed Cyclic	51.2	2.99	2ϕ16	397.2	1.805
S2-4R	Reversed Cyclic	58.02	3.33	2ϕ16	397.2	1.805

3.5 Test Procedure

Test program is divided into monotonic and reversed loading. For revered loadings, the test beams were over turn upside down manually as Fig.3-5. From the test, it can be realizes that experimental set-up was important to control the precision of mid-span deflection. The load-unload paths were according to following stage: flexural crack, diagonal shear crack, and first yield of tension steel. After this first yield, control displacement was applied.

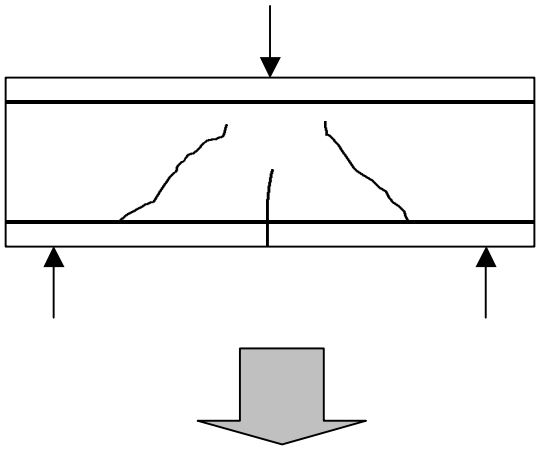

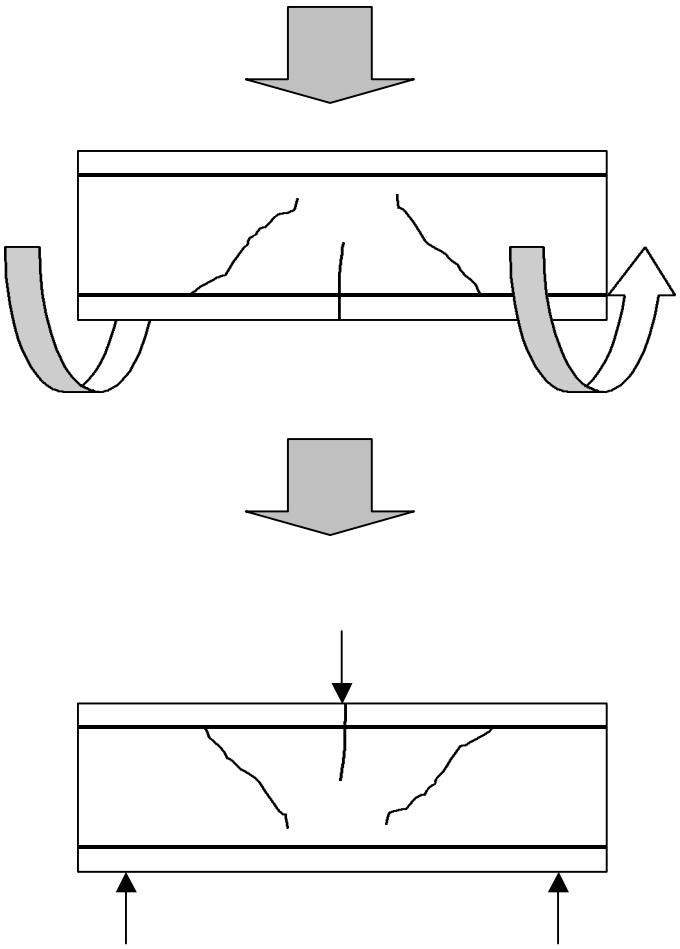

Fig. 3-5 Over turn upside down manually for reversed loading

CHAPTER 4

NUMERICAL PROCEDURE

4.1 Analytical Procedure

Finite element program, WCOMD-SJ, which had been developed at the University of Tokyo, was used in this numerical analysis. The analytical program is mainly composed of programs *WCOMRA* and *WCOMRC* (Fig. 4.1). [5] The main function and sub-program are explained as follow

WCOMRA: This part is deals with the input process. Input data are the dimensional shapes of the member composed of elements and the nodal data, and material properties e.g. the elastic modulus and yield strength of reinforcement, and the compressive strength.

WCOMRC: This is the main part, which reads nodal forces, nodal displacement, incremental loads and indices for structuring the total matrix, and executes the analysis by using the element data.

INPUTG: This sub-program reads the data of nodes, elements, and loads from the input data file, arrange them and writes the indices for the data and overall stiffness matrix on an external file.

MGN: This sub-program reads the external data, calculates the *B matrix* in the form of strain-node displacement matrix, and writes the calculated results on an external file.

DISPI: This sub-program initializes the data files for execution of program WCOMRC.

MTRLRC: This sub-program describes the reinforced concrete plate element model.

MTRLJO: This sub-program describes the reinforced joint element model. MTRLRC and MTRLJO calculate stress from strains of each element, and give the value D matrix, which is necessary to construct the stiffness matrix for convergence process to the main routine.

MTRLEL: This sub-program describes the elastic material model.

PRINST: This sub-program writes calculated stress and strain on an external file.

WCOMRDM: This post-processing program process nodal displacements and express output in the form of load-displacement relationship.

WCOMRGP: This is another post-processing program, which process deformation of shapes, stress distribution, strain distributions, crack pattern and failure modes are graphically output.

4.2 In-Plain Constitutive Models of Reinforced Concrete

4.2.1 Model of Uncracked Concrete

The analytical model for concrete prior to cracking is constructed based on elasto-plastic and fracture model [5].

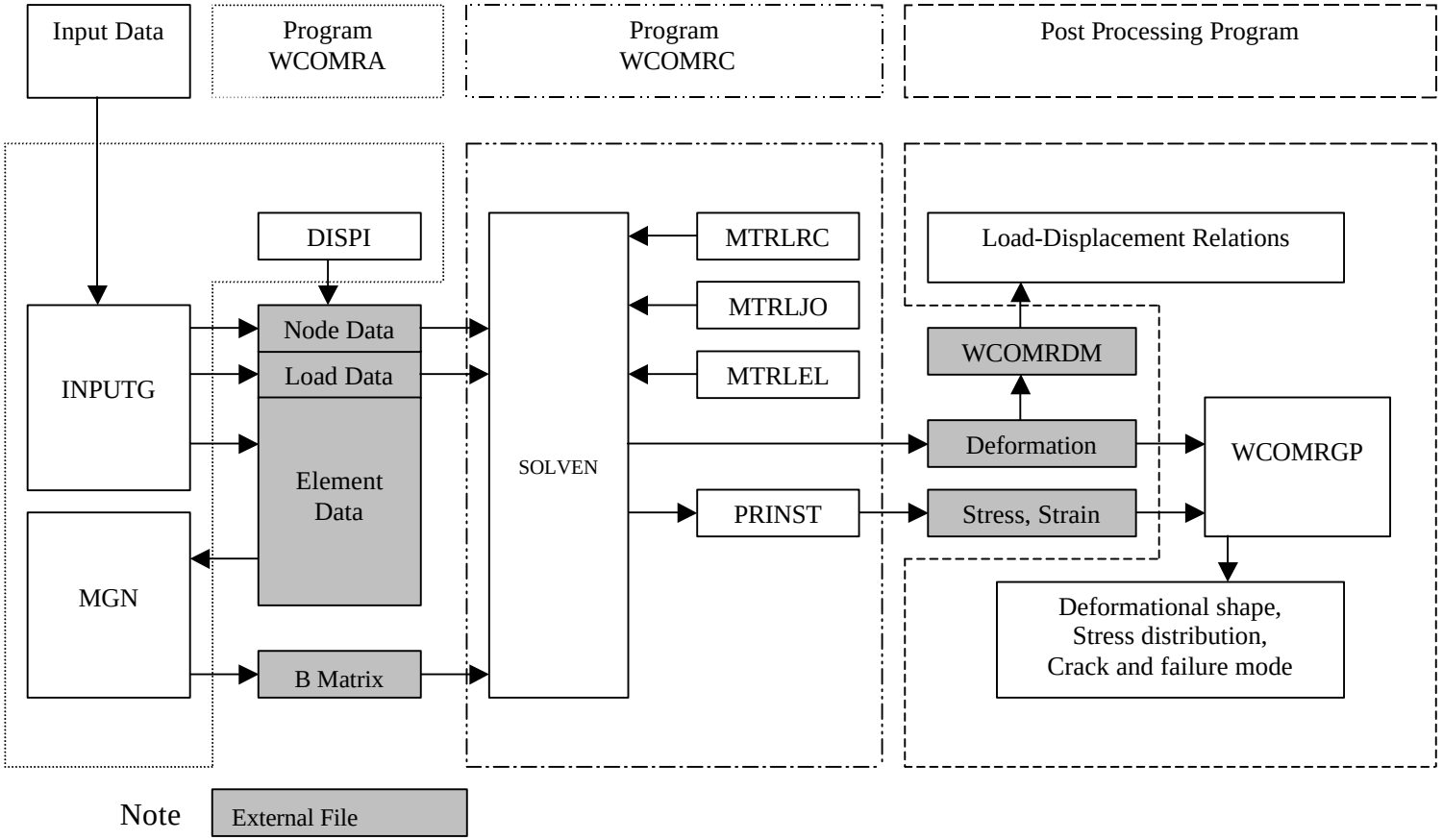

Fig. 4-1 Structure of WCOMR

Fig. 4-2 gives the schematic outline of elasto-plastic and continuum fracturing system [10]. Concrete elasticity is modeled as spring while concrete plasticity is modeled as sliders. The damage in concrete is modeled as broken springs, which is irreversible process. Total stress is assembled from the internal stress, which develop over the non-damaged elasto-plastic components. Then elastic strain is proportional directly to internal stress intensity, which applies over these non-damage elatio-plastic components.

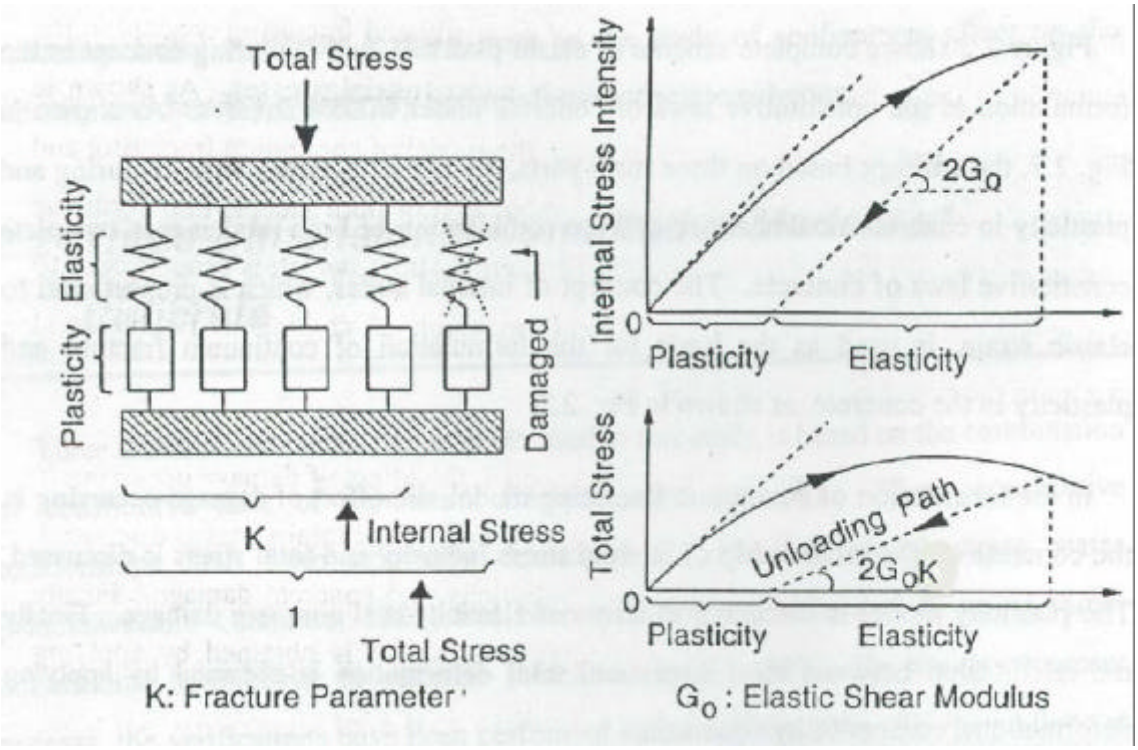

Fig. 4-2 Schematic outline of elasto-plastic and continuum fracturing system

Therefore elastic strain is selected to represent the internal stress intensity that governs the plasticity and fracturing in the concrete continuum. The index namely *fracture parameter, K*, is introduced to represent the ratio of non-damage components, which can carry the stress in concrete. The relationship between equivalent stress S and equivalent strain E is formulated with initial elastic modulus E_0=2, fracture parameter K, and equivalent plastic stain E_P as shown in Fig. 4-3. The equivalent plastic strain E_P and fracture parameter have been formulated solely with the maximum equivalent total strain as defined in Fig.4-4.

The advantage of this model is the capability to cover any loading history, including unloading and reloading in biaxial stress states, which use one unique mathematical expression.

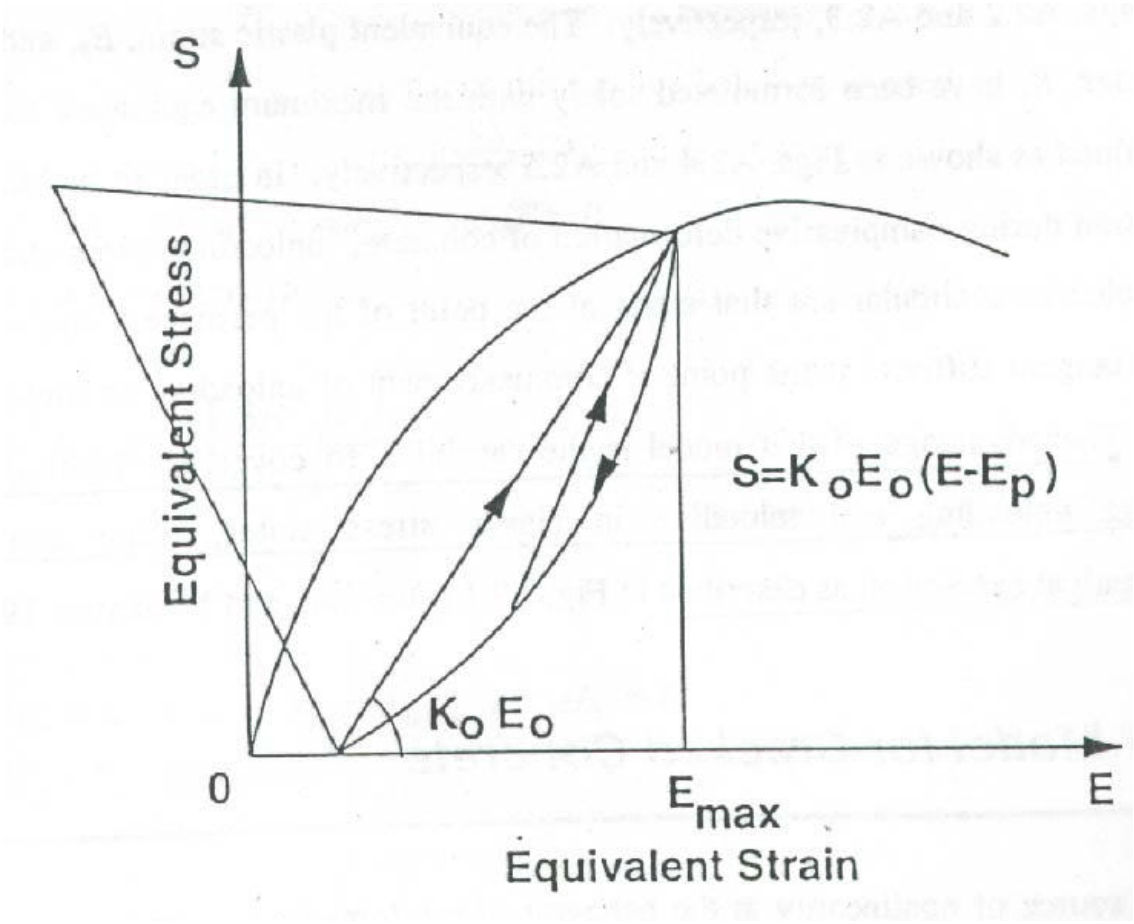

Fig. 4-3 Uncracked concrete modeling, which express in the term of equivalent stress S, equivalent strain E and initial elastic modulus E_0

The definition of equivalent stress and equivalent strain are express as follow

Equivalent Stress: $S = \sqrt{(a\sigma_m)^2 + (b\tau_d)^2}$

a: constant = 0.6/fc' b: constant =1.3/fc'

fc': Maximum compressive stress

σ_m : *Average stress*

$$= \sqrt{2}\frac{\sigma_1 + \sigma_2}{2}$$

τ_d : *Deviation stress*

$$= \sqrt{2}\frac{\sigma_1 - \sigma_2}{2}$$

σ_1 and σ_3 : Principal Stresses; $\sigma_1 > \sigma_3$

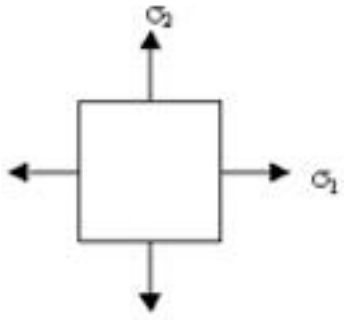

$$\text{Equivalent Strain}: \quad E = \sqrt{(c\varepsilon_m)^2 + (d\gamma_d)^2}$$

c: constant $= 0.62/\varepsilon'_{co}$

d: constant $= 0.98/\varepsilon'_{co}\,dfa$

ε'_{co}: Compressive strain for fc`

ε_m : *Average strain*

$$= \sqrt{2}\,\frac{\varepsilon_1 + \varepsilon_2}{2}$$

γ_d : *Deviatoric strain*

$$= \sqrt{2}\,\frac{\varepsilon_1 - \varepsilon_2}{2}$$

ε_1 and ε_1 : Principal Strain; $\varepsilon_1 > \varepsilon_2$

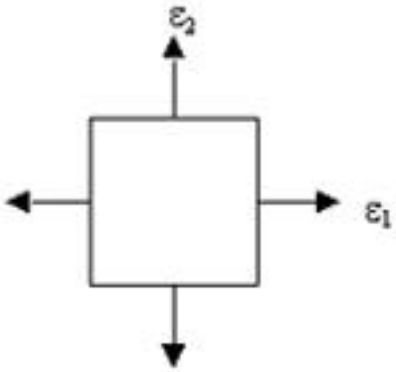

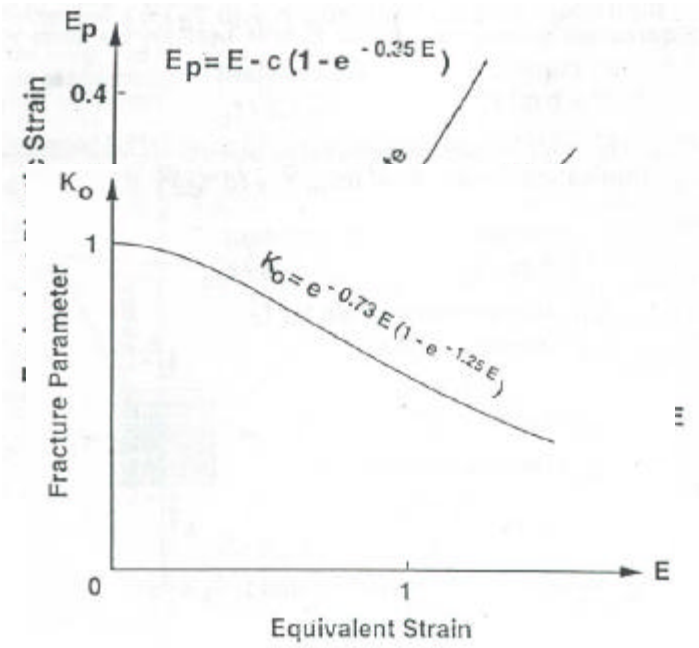

Fig. 4-4 Mathematical definition of equivalent plastic strain E_P and fracture parameter K

4.2.2 Model of Crack Concrete

4.2.2.1 Crack Concrete in Tension

Tension failure of concrete is accompany with growth crack. After forming of crack, concrete in the crack plain cannot carry tensile force. In between crack concrete, concrete still continue carry tensile force by transmitting to reinforcing bar through bond action. This phenomena is known as tension stiffening. The model of concrete under tensile stress is independent of the spacing of cracks, the direction of reinforcing bar and reinforcement ratio. Therefore the model is formulated in the term of average stress and average strain as shown in Fig. 4-5.

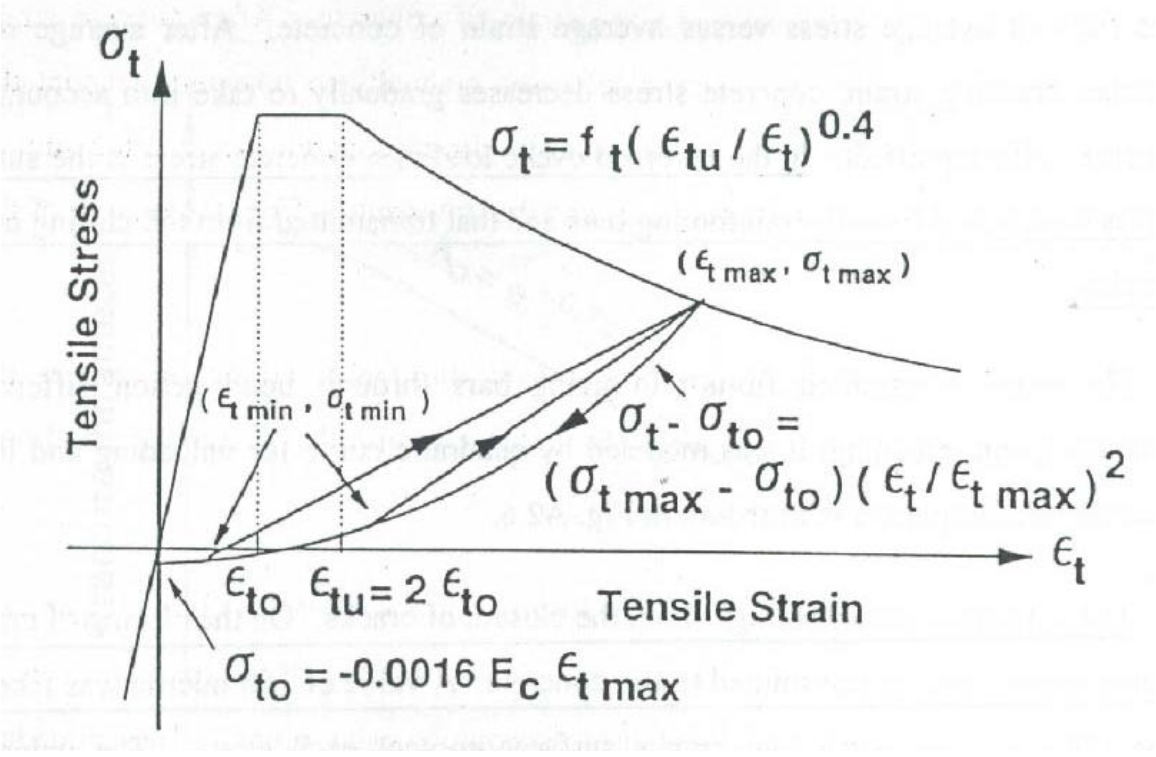

Fig. 4-5 Stress transfers through bond action.

In the reversed loading, the former crack will close. Hence concrete stress can transmitted both to main reinforcing bar and these close crack. The unload process will bring surface of crack contact each other. A tensile strain of 150×10^{-6} had been given for this mechanism. (Fig. 4-6)

4.2.2.2 Crack Concrete in Compression

The main factor that reduces compressive strength of concrete in two dimensions is transverse strain. This concrete softening effect can account in the model by reducing fracture parameter K of uncracked concrete as a function of the tensile strain, which perpendicular to crack. (Fig. 4-7)

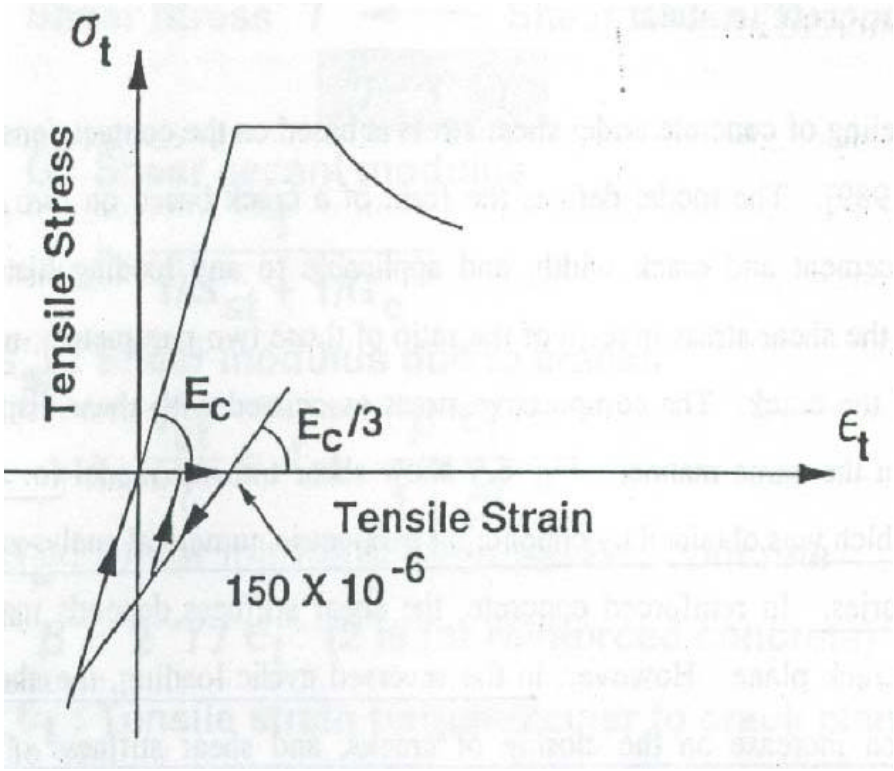

Fig. 4-6 Stress transfer by closing of crack

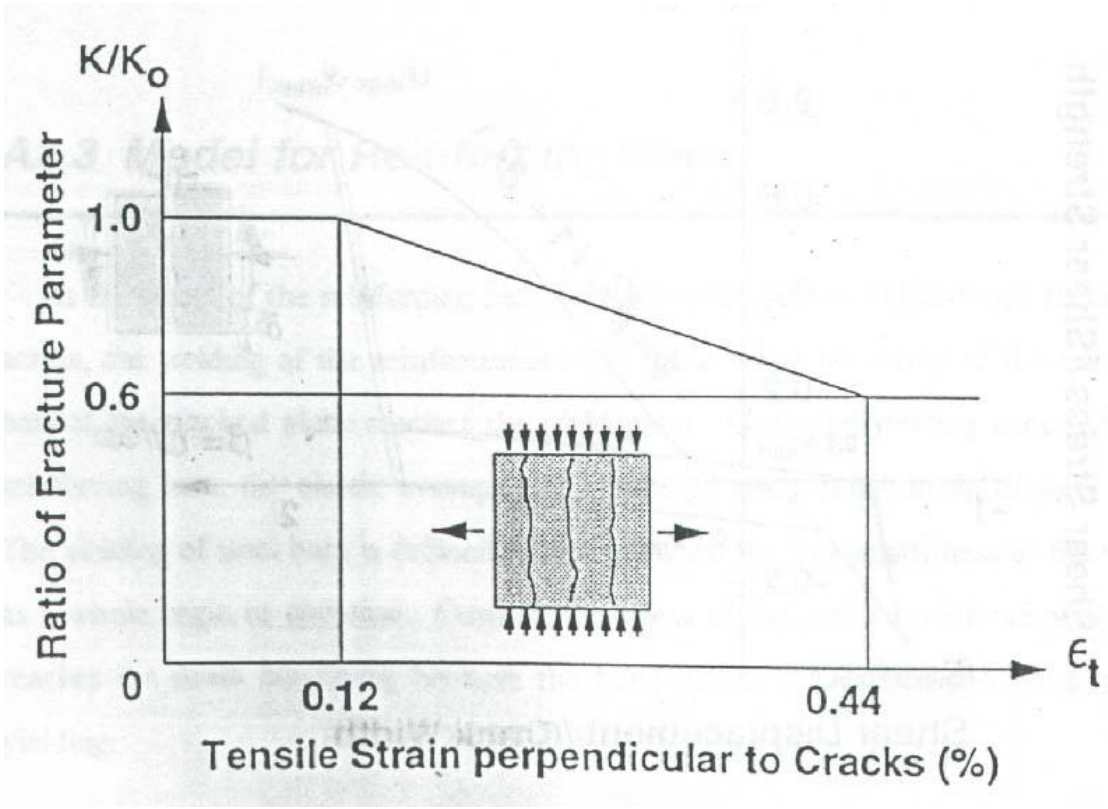

Fig. 4-7 Reduction in fracture parameter due to concrete softening as function of tensile strain perpendicular to crack

4.2.2.3 Crack Concrete in Shear

The modeling of concrete under shear stress is based on contact density function (Li, et. al, 1989). The model is formulated based on two parameters; shear displacement, δ, and crack width, ω, and applicable to any loading history. In reinforced concrete, the shear stiffness is depending mainly on the stiffness of crack plain.

In reversed loading, closing of the crack will increase shear stiffness of crack plain. Uncracked concrete portion should be contributed to increase shear stiffness. Parametric numerical analysis for any loading condition had been conducted to obtain thear model as shown in Fig. 4-8.

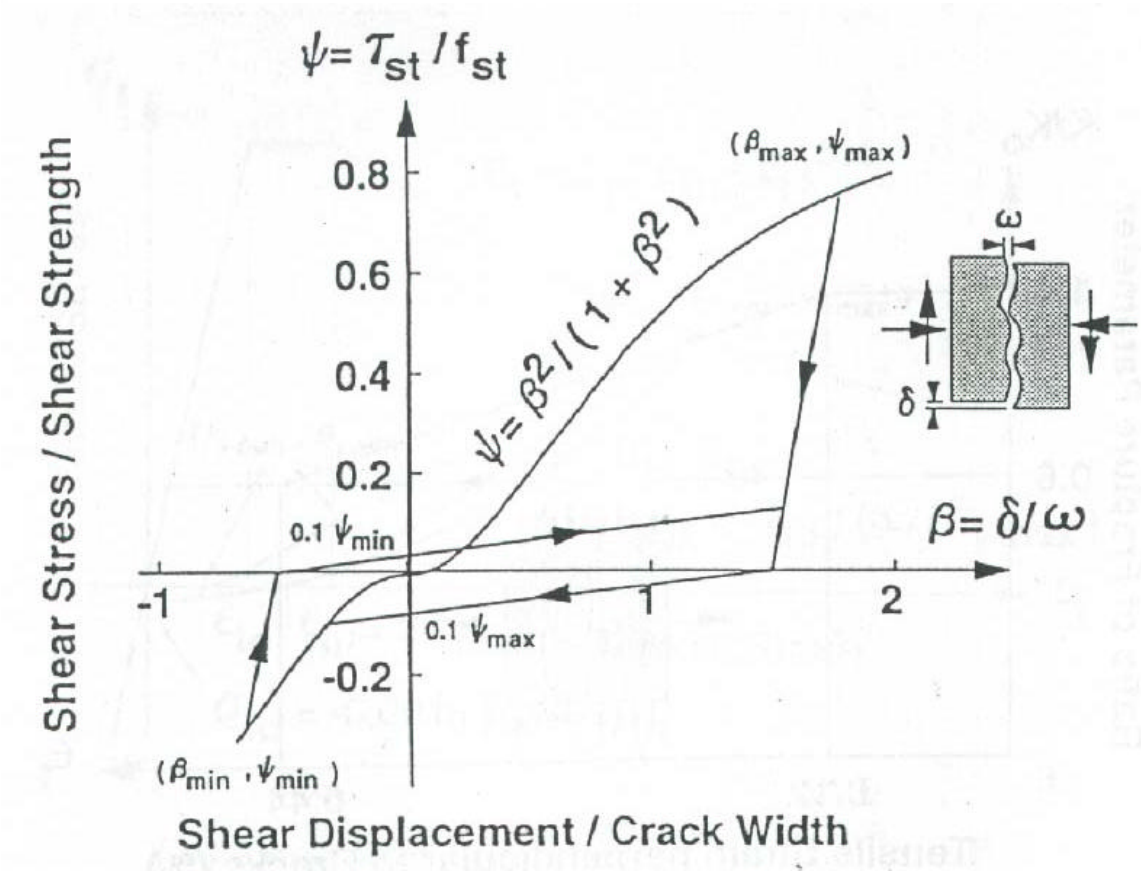

Fig. 4-8 Simplified shear transfer model.

The formulation of shear stress and shear strain are defined as follow:

Shear Stress τ $\leftarrow$ *Shear Strain* γ

$$\tau = G\gamma$$

G: Shear second modulus

$$= \frac{1}{\frac{1}{G_{st}} + \frac{1}{G_C}}$$

G_{st}: Shear modulus due to crack

$$= \frac{\tau_{st}}{\gamma} = f_{st}\frac{\beta\varepsilon_t}{1+\beta^2}$$

G_C: Shear modulus of uncracked concrete

$$\beta = 2\frac{\gamma}{\varepsilon_t}$$

ε_t : Tension strain perpendicular to crack plain

f_{st} : Shear transfer strength

CHAPTER 5

EXPERIMENTAL RESUTLS AND NUMERICAL ANALYSIS

5.1 Experimental Results and Discussion

To confirm the consistency of the test, three RC beam in series 1 and two RC beam in series 2 subjected to monotonic loading were executed and the experimental results with crack pattern are shown as follow

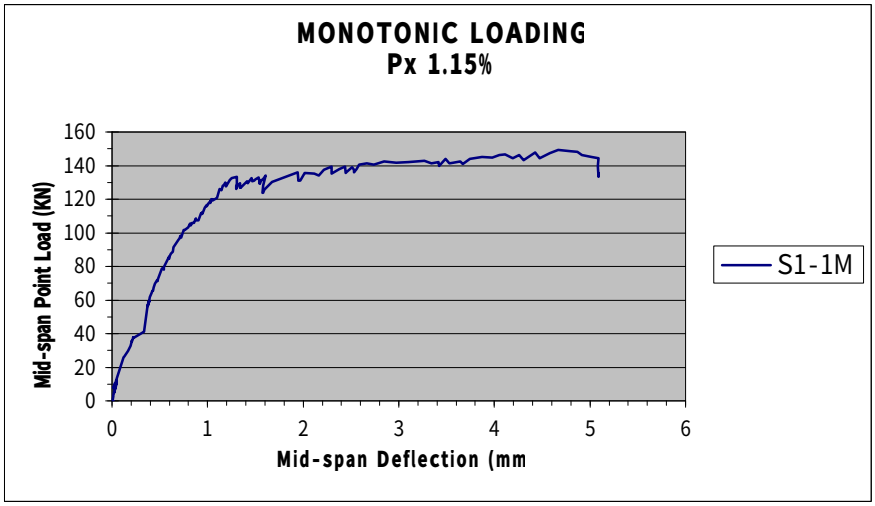

Fig. 5-1 Mid-span deflection of specimen S1-1M under monotonic loading

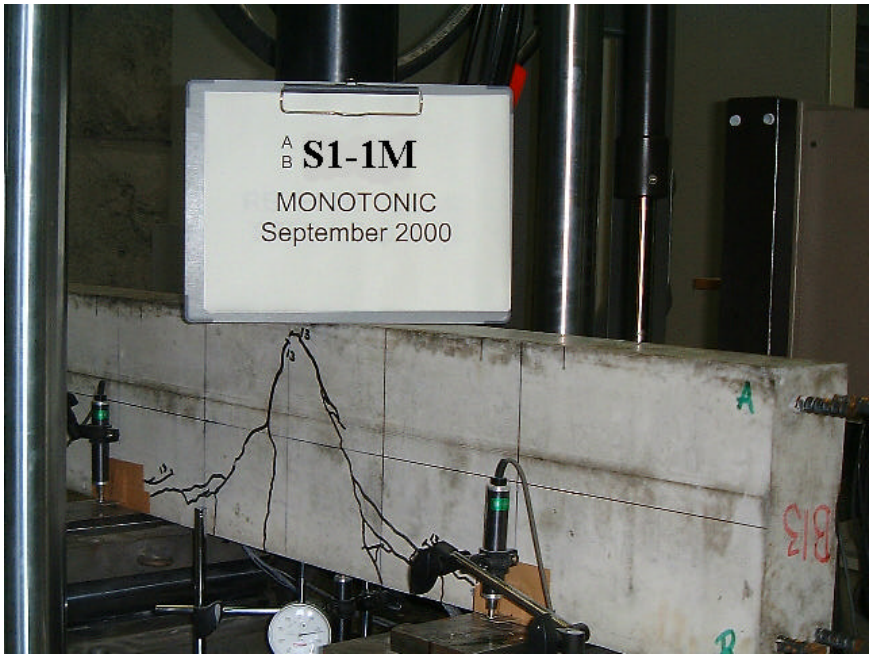

Fig. 5-2 Crack pattern of specimen S1-1M under monotonic loading

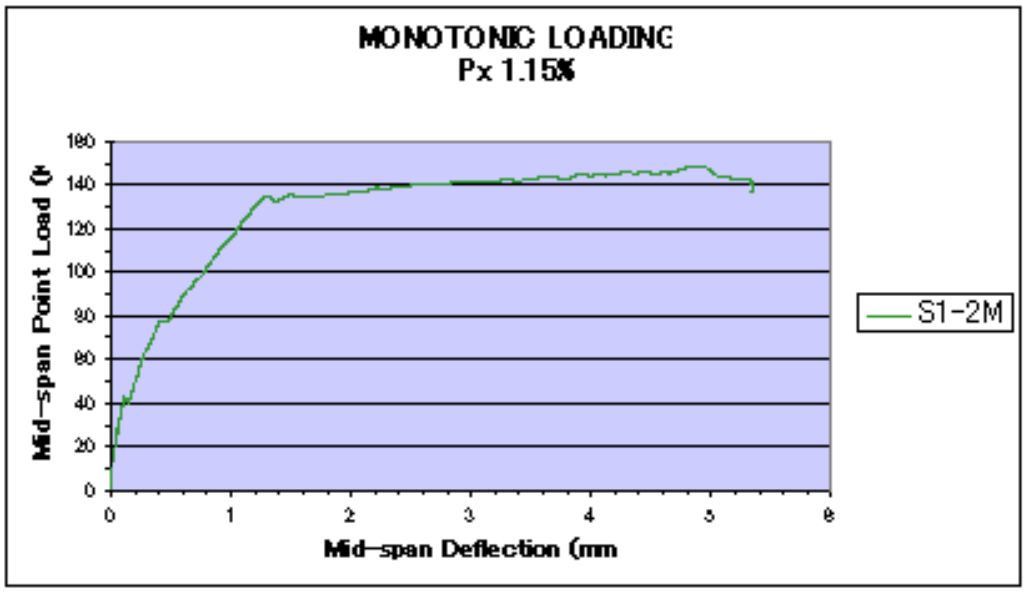

Fig. 5-3 Mid-span deflection of specimen S1-2M under monotonic loading

Fig. 5-4 Crack pattern of specimen S1-2M under monotonic loading

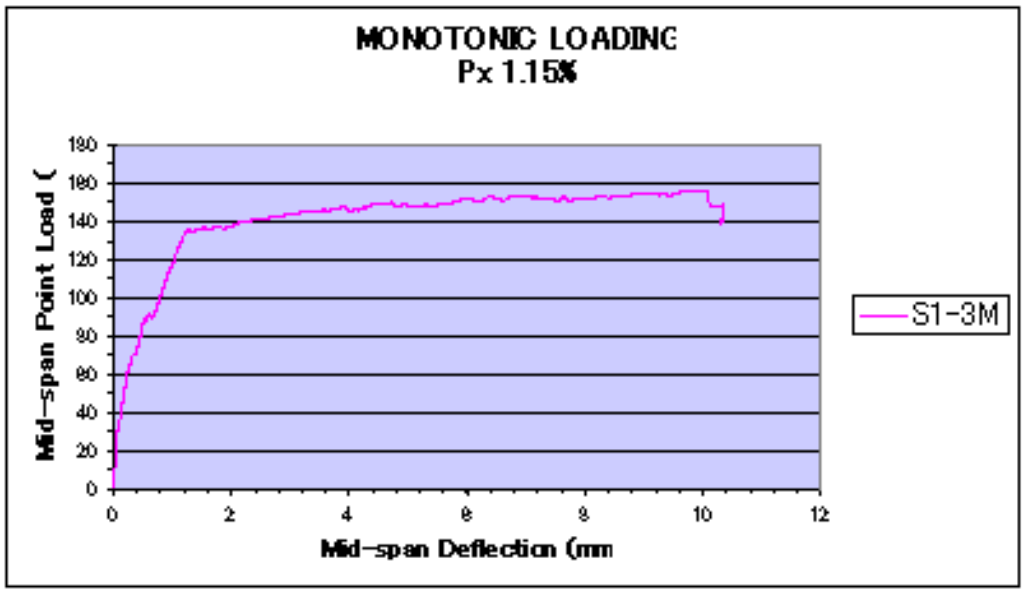

Fig. 5-5 Mid-span deflection of specimen S1-3M under monotonic loading

Fig. 5-6 Crack pattern of specimen S1-3M under monotonic loading

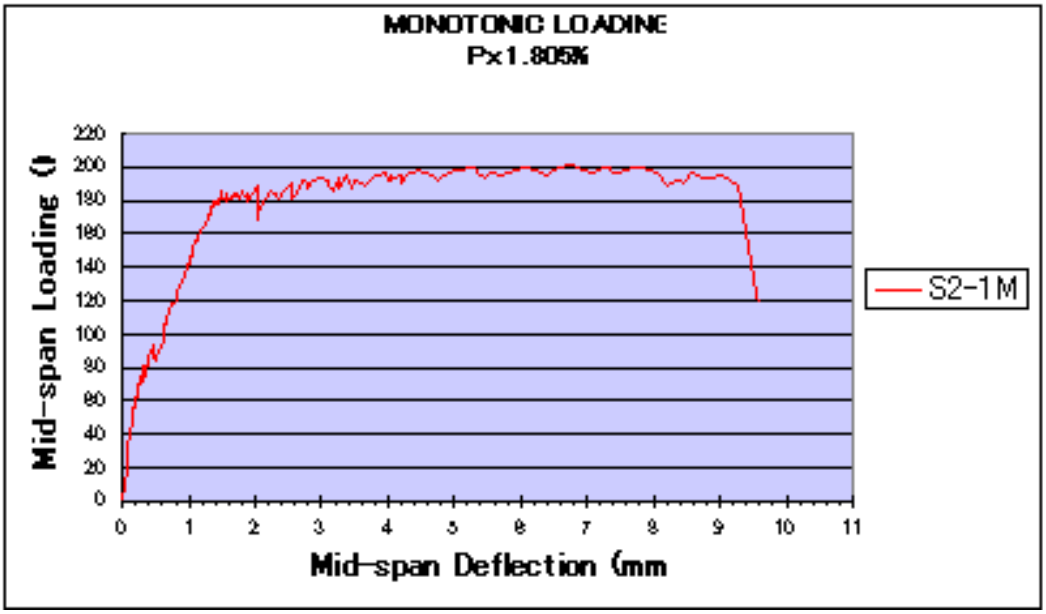

Fig. 5-7 Mid-span deflection of specimen S2-1M under monotonic loading

Fig. 5-8 Crack pattern of specimen S2-1M under monotonic loading

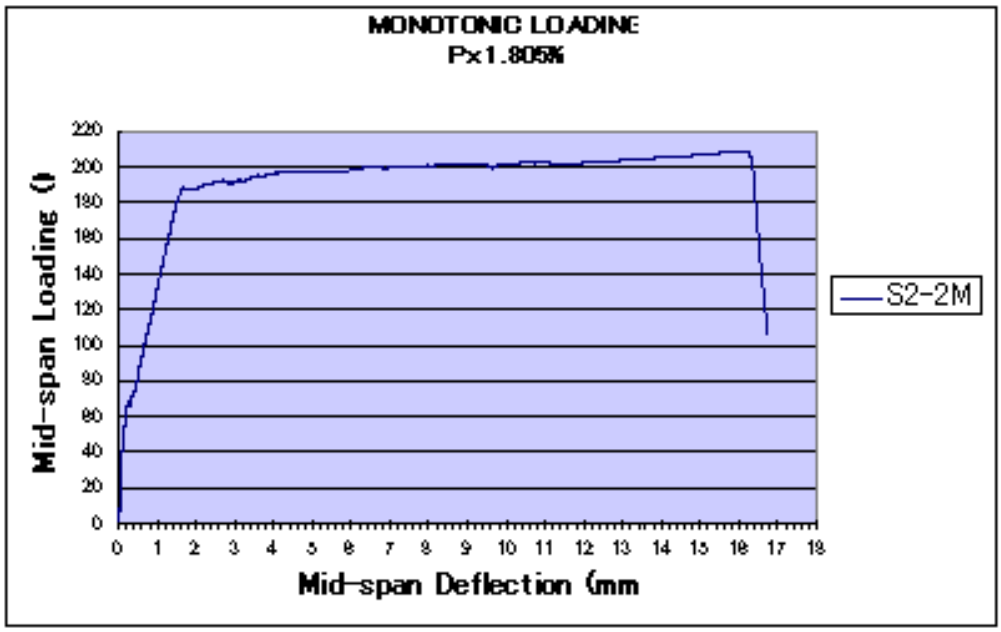

Fig. 5-9 Mid-span deflection of specimen S2-2M under monotonic loading

Fig. 5-10 Crack pattern of specimen S2-2M under monotonic loading

For reversed loading, two beam specimens in series 1 and two beam specimens in series 2 were shown as follow

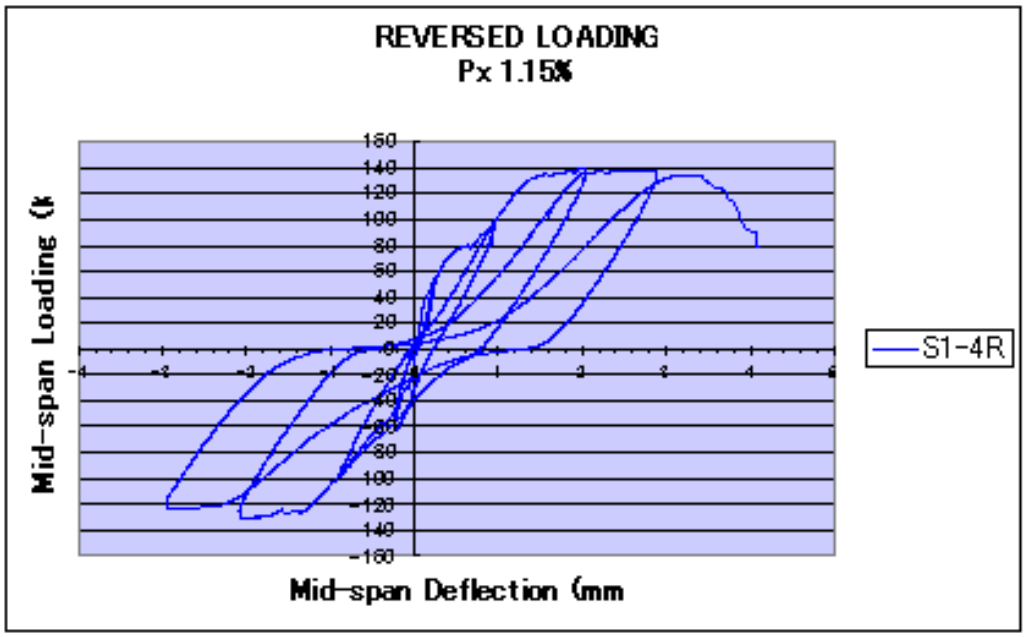

Fig. 5-11 Mid-span deflection of beam specimen S1-4R under reversed loading

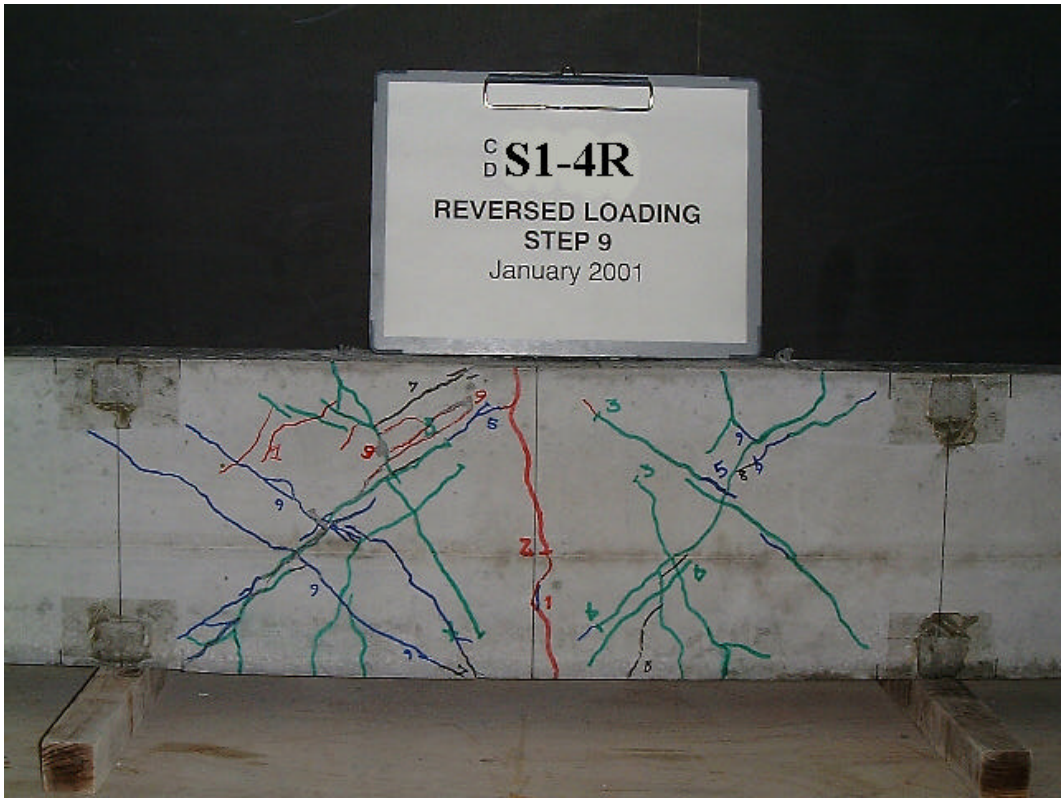

Fig. 5-12 Crack Pattern of specimen S1-4R under reversed loading

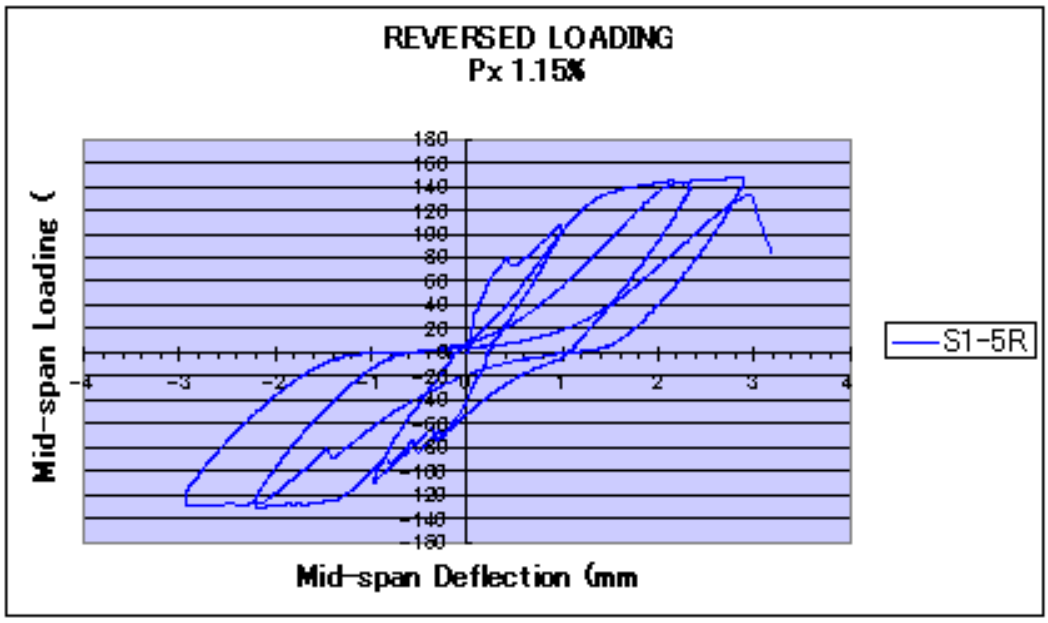

Fig. 5-13 Mid-span deflection of beam specimen S1-5R under reversed loading

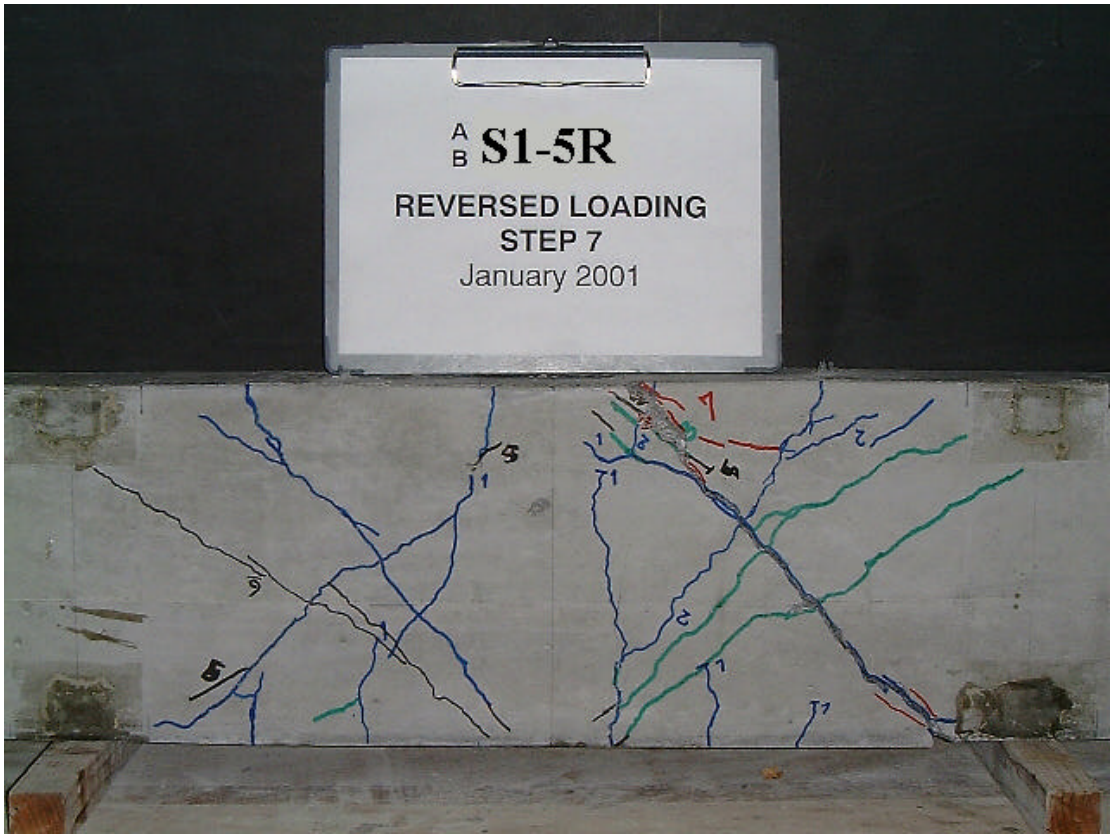

Fig. 5-14 Crack Pattern of specimen S1-5R under reversed loading

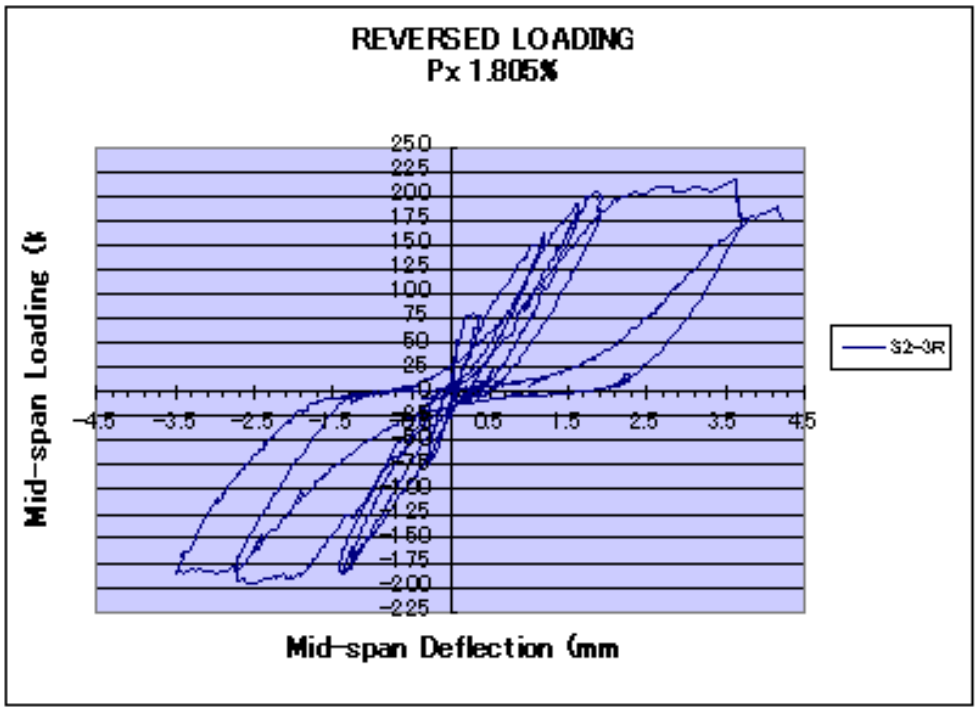

Fig. 5-15 Mid-span deflection of beam specimen S2-3R under reversed loading

Fig. 5-16 Crack Pattern of specimen S2-3R under reversed loading

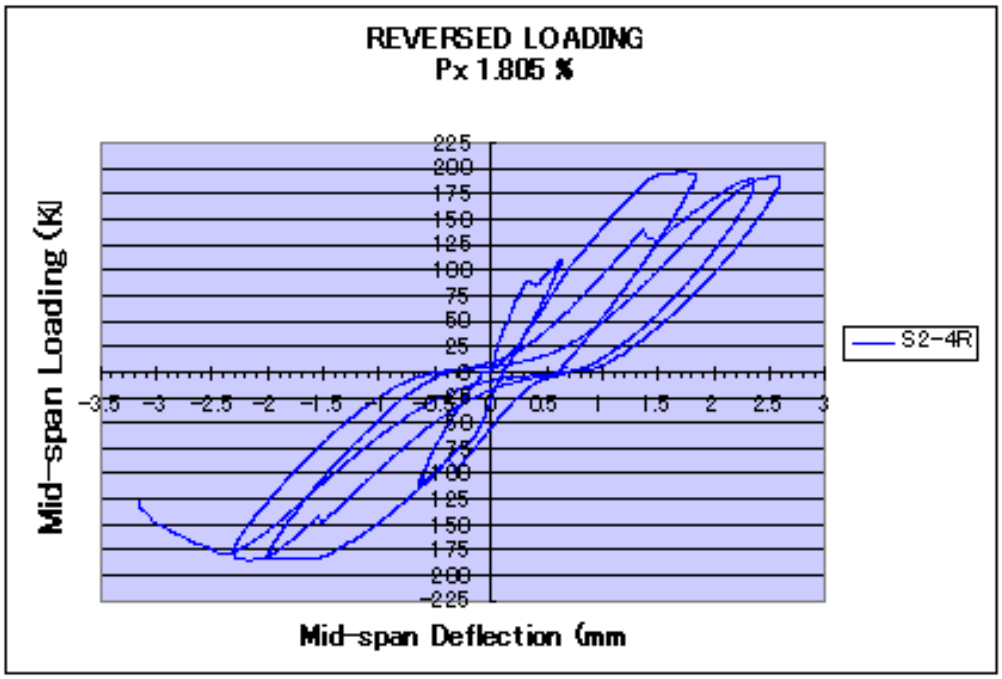

Fig. 5-17 Mid-span deflection of beam specimen S2-4R under reversed loading

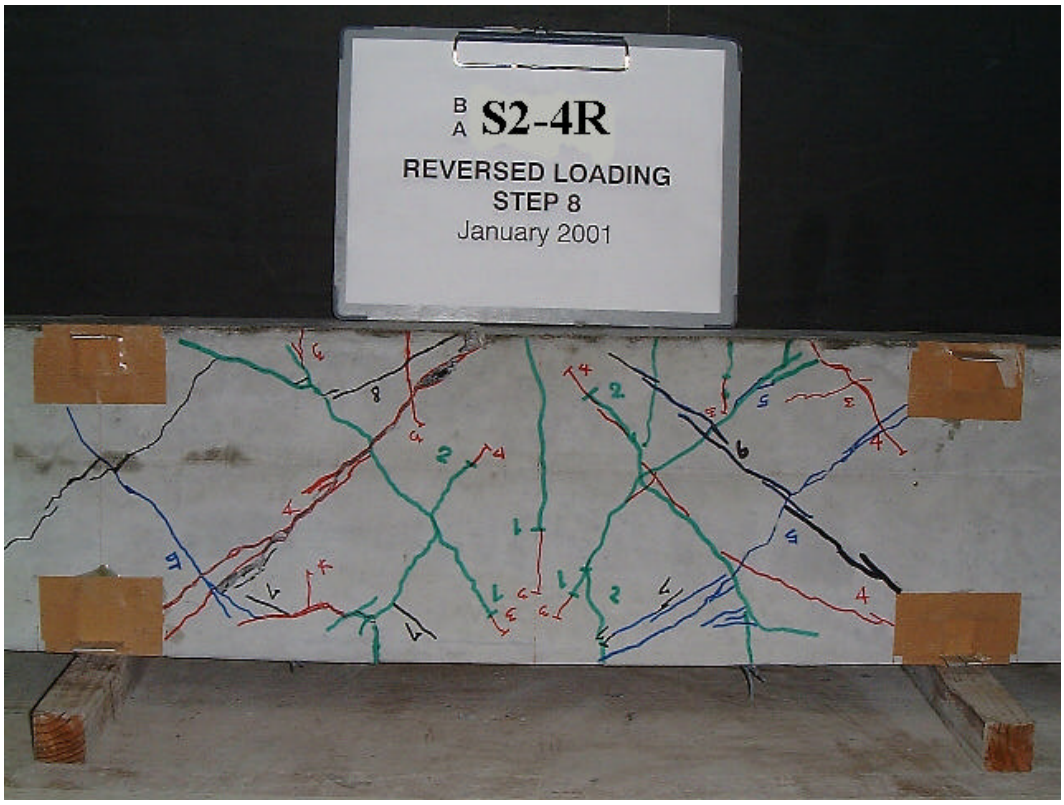

Fig. 5-18 Crack Pattern of specimen S2-4R under reversed loading

Under monotonic loading, three beam specimens in series 1 and two beam specimens in series 2 were combined in Fig. 5-19 and 5-20 respectively.

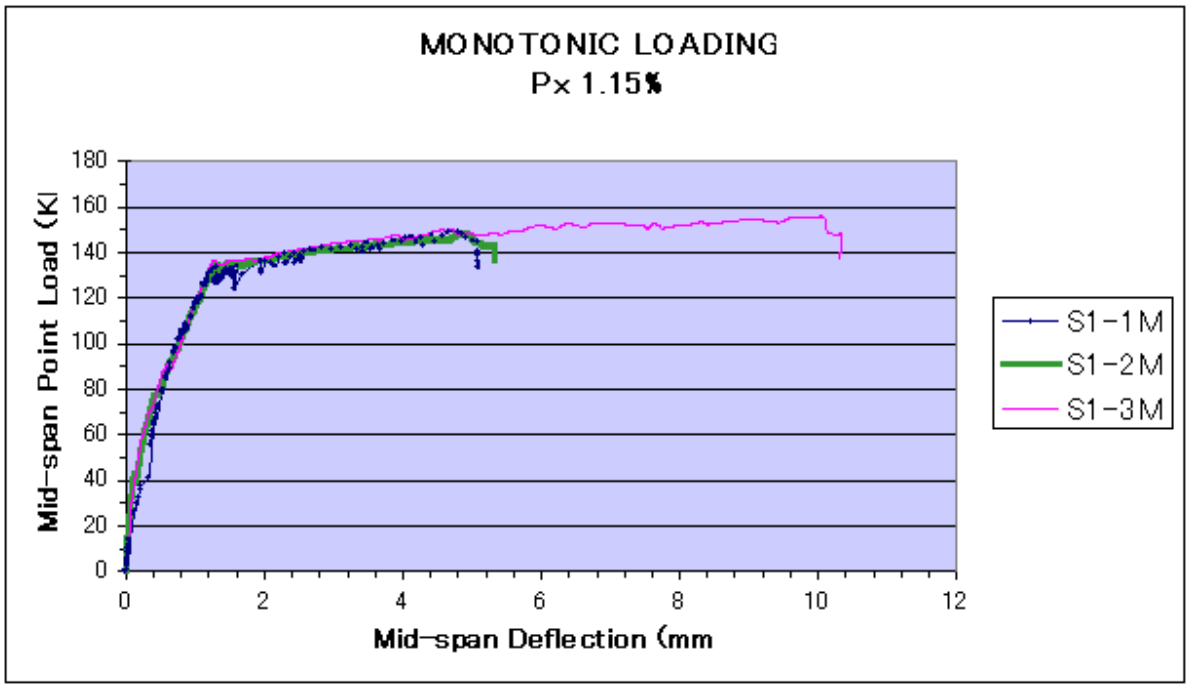

Fig. 5-19 Mid-span deflection under monotonic loading of beam in series 1

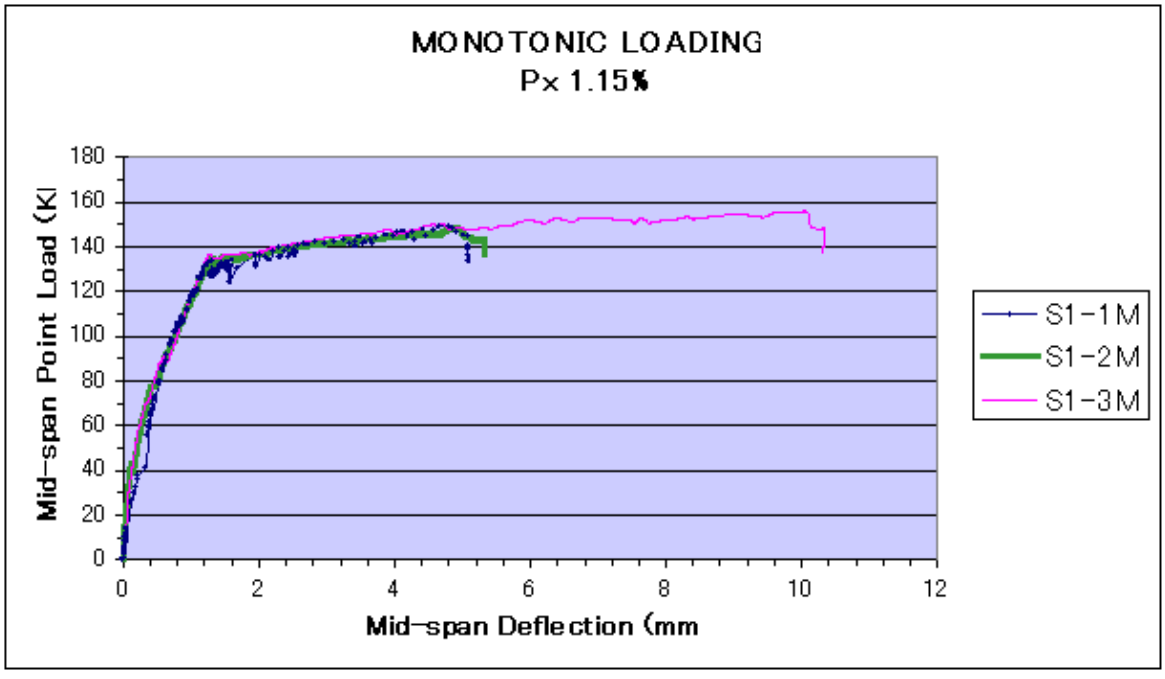

Fig. 5-20 Mid-span deflection under monotonic loading of beam in series 2

In series 1, for monotonic loading, three beam specimens show well agreement of first yield at 135 KN. After yielding of main reinforcing bar, load capacity gradually increase until reach ultimate load due to strain hardening effect. These three beams specimens have different compressive strength of concrete as follow 52.2, 52.7, and 57.18 for specimen S1-1M, S1-2M and S1-3M, respectively. Shear capacity of RC beam without web reinforcement should be depend greatly on web concrete compressive strength. Therefore the difference on ultimate load should come from the difference in concrete compressive strength. However to quantitative how much for these effect, normal concrete and high strength should be conducted to compare with these existing data. Another possible effect is environmental temperature, which affect creep and plastic strain. Specimen S1-1 and S2-1 was tested in summer season (average temperature is 25^{o}), while the rest were tested in winter season (average temperature is 5^{o}). The temperature difference is approximately 20^{o}.

In series 2, for monotonic loading, two beam specimens show well agreement of first yield at 188 KN. The ultimate load is slightly different as similar as in series 1. However, in safe side, specimen S2-1M, which has lower ultimate load, should be selected.

From experimental in series 1 and 2 show that higher reinforcement ratio will increase ultimate load and deflection under monotonic loading. In this case, increasing of reinforcement ratio from 1.15% in series 1 to 1.805% in series 2 by 57% will increase ultimate deflection by 76%.

For reverse loading, the experimental results show that first yield load of RC beam subjected to reversed loading is identical to that one subjected to monotonic. The cross diagonal cracks in web concrete is not affect the first yield load because the crack, which occur from load in opposite direction, will close as shown in Fig. 5-21.

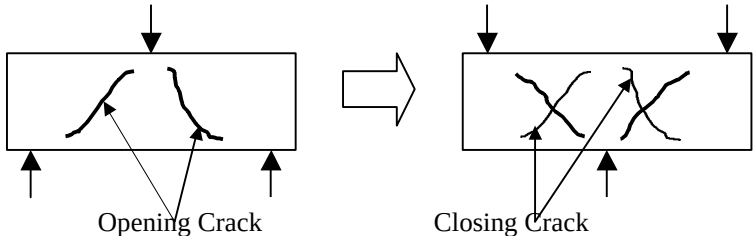

Fig. 5-21 Closing crack in reversed loading.

The opening and closing of cracks will cause a deterioration of the concrete resulting in stiffness degradation.

For reversed loading, the ultimate load is almost the same yield load as same as monotonic but significant lower ultimate deflection. To compare this ultimate deflection, ductility, which expresses the element capacity to undergo inelastic behavior and absorb energy, is appropriate to use. Several forms of ductility are available. In this study, displacement ductility was investigated.

Displacement ductility factor, μ, is defined as the ratio of deflection at the ultimate load to the deflection at first yield of the tension steel. [4]

$$\mu = \frac{\delta_{Ultimate}}{\delta_{Yield}}$$

According to above definition, displacement ductility factor of all specimens are shown in Table 5-1.

Table 5-1 Displacement ductility factor of all specimens

Specimen No.	Load Pattern	ρ (%)	Yield Deflection mm	Failure Deflection mm	Ductility Factor $\delta_{Ultimate}/\delta_{Yield}$
S1-1M	Monotonic	1.15	1.3	5.1	3.9
S1-2M	Monotonic	1.15	1.3	5.3	4.1
S1-3M	Monotonic	1.15	1.3	10.1	7.8
S1-4R	Reversed	1.15	1.4	3.3	2.4
S1-5R	Reversed	1.15	1.4	3.0	2.1
S2-1M	Monotonic	1.805	1.5	9.0	6.0
S2-2M	Monotonic	1.805	1.6	16.3	10.2
S2-3R	Reversed	1.805	1.9	4.1	2.2
S2-4R	Reversed	1.805	1.6	3.1	1.9

For reinforcement ratio 1.15%, the effect of reversed loading will decrease displacement ductility factor by 38% while that one for reinforcement ratio 1.805% will decrease by 63%.

5.2 Effective Size of RC Zone

The size of RC zone in the finite analysis has an effect directly on stiffness of member. The past research by An X. proposed that size of RC effective zone is related to the bond characteristic of reinforcing bar as Fig. 5-22. [2,3]

After the forming of crack, stress in concrete will transfer to steel bar. Hence larger concrete covering is earlier yield of steel bar. If the area of concrete is too large, the stress increase should be limit to yield strength of steel bar. Hence the maximum size of concrete zone for one certain bar can express as

$$A_{C,max} f_t = A_S f_y$$

$$A_{C,max} = \frac{A_S f_y}{f_t}$$

where A_S : area of steel bar,
$A_{C,max}$: maximum area of bond effect zone in concrete
f_y: yielding strength of steel bar.

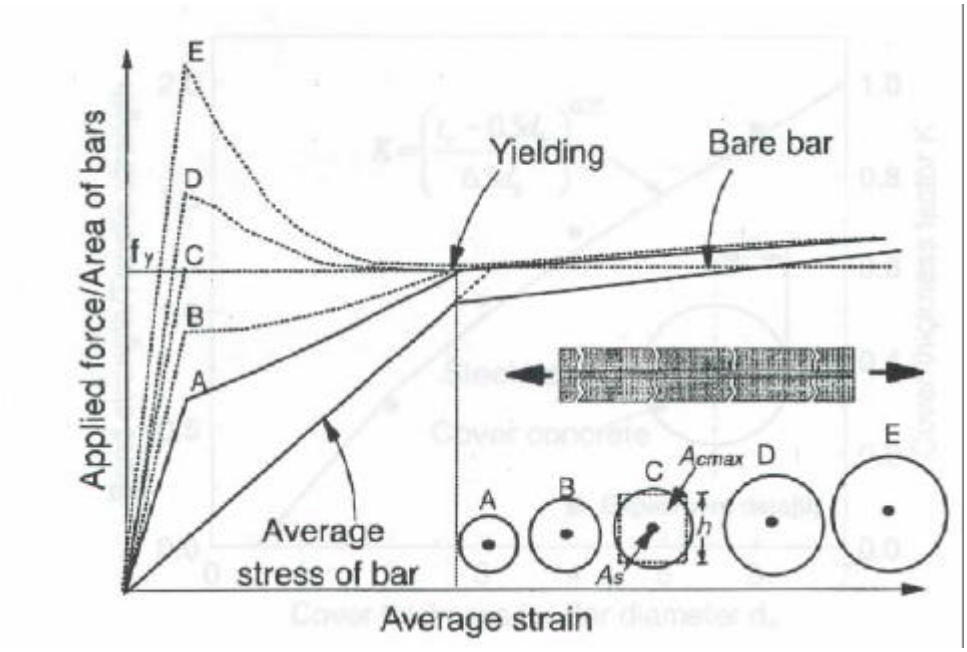

Fig.5-22 Crack control capability and concrete area.

In the two dimensional finite element computations, equivalent maximum area of bond effect zone, $A_{C,\,max}$ from circular shape to RC zone height as Fig. 4-7 is suitable to implement as follow

$$A_{C,\max} = h_{\max}^{\,2}$$

$$h_{\max} = \frac{\sqrt{\pi}}{2} \cdot d_b \sqrt{\frac{f_y}{f_t}}$$

Hence the height of RC zone used in computation is

$$h = \frac{h_{\max}}{2} + tc \quad , tc < h_{\max}$$

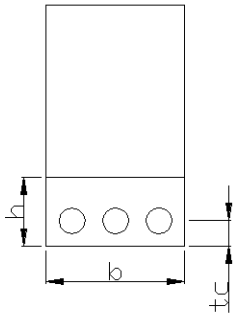

Fig. 5-23 The height of RC zone in computation

5.3 Analytical Results

Finite element program namely WCOMD, which had been developed in the University of Tokyo, was used in this analysis. Effective size of RC zone according to An X., 1996, had been implement. RC element and plain concrete element in FE modeling of specimen S1-2M are shown in Fig. 5-24

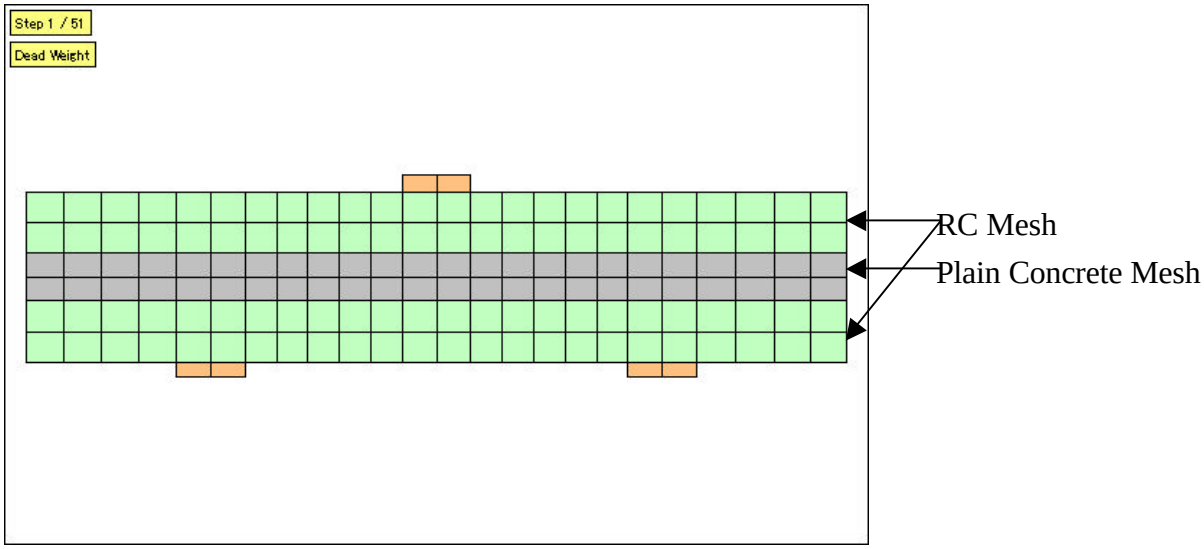

Fig. 5-24 RC zone and PL zone of FE modeling of specimen S1-2M

The analytical result of specimen S1-2M is compare to experimental result as shown in Fig. 5-25.

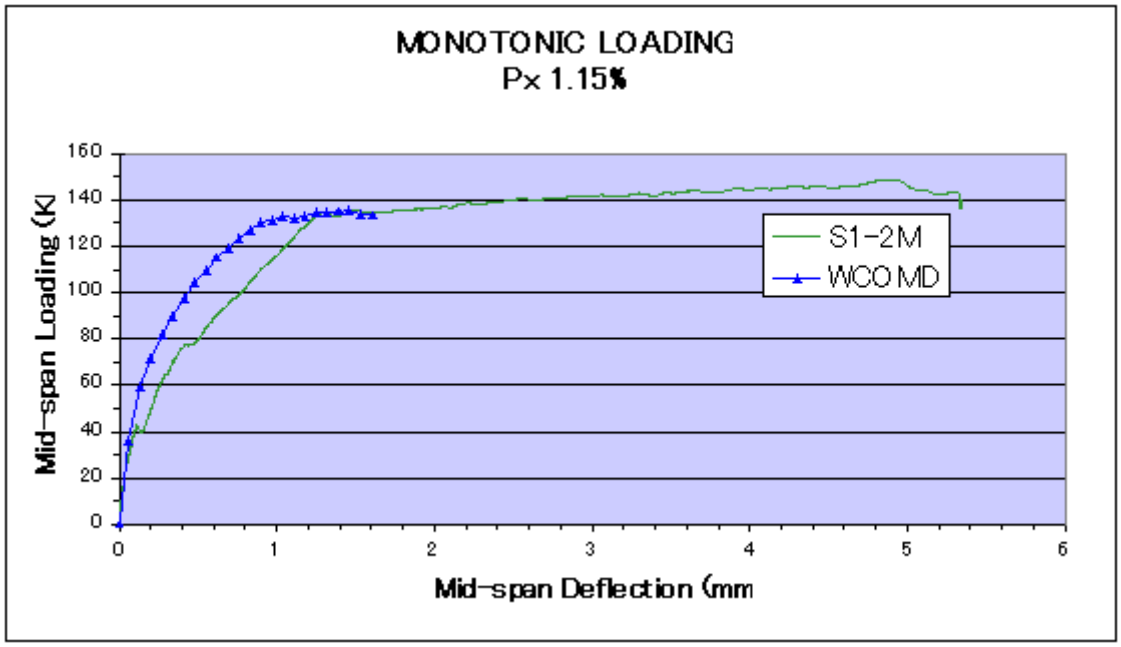

Fig. 5-25 Comparison of analytical and experimental results.

The crack pattern of analytical and experimental is shown in Fig. 5-26 and 5-27.

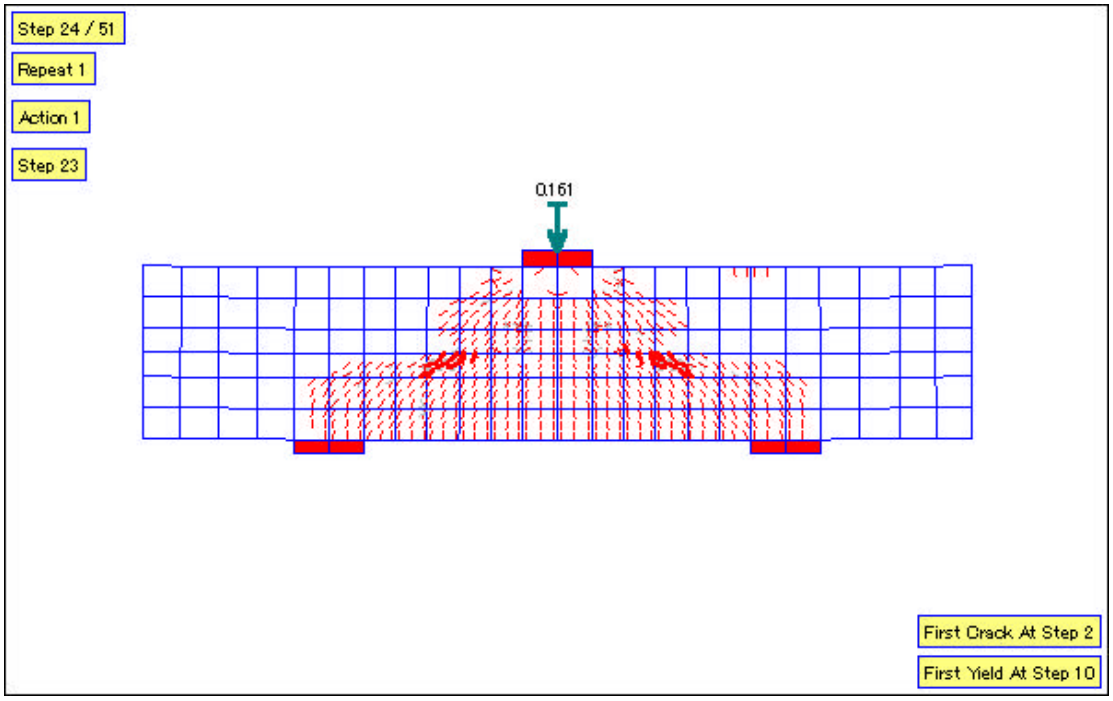

Fig. 5-26 Crack pattern of analytical result of specimen S1-2M

Fig. 5-27 Crack pattern of experimental result.

For series 2, specimen S2-1M, which has lower ultimate load, was selected for safe side to model. RC element and plain concrete element in FE modeling are shown in Fig. 5-28

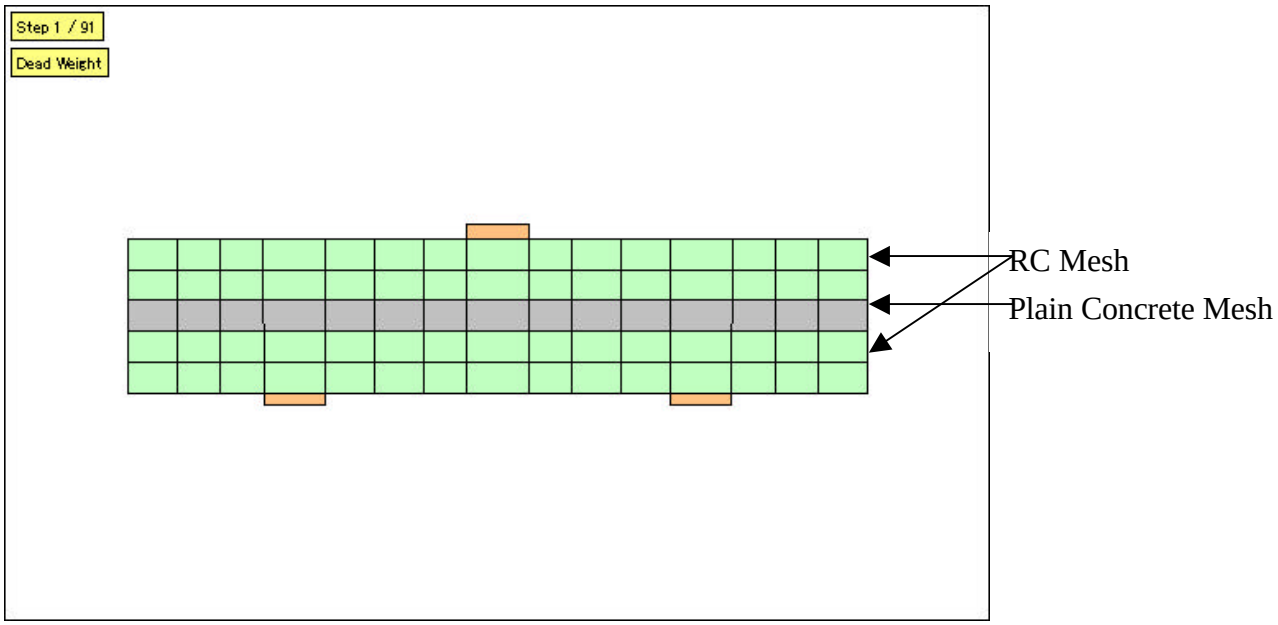

Fig. 5-28 RC zone and PL zone of FE modeling of specimen S2-1M

The analytical result of specimen S1-2M is compare to experimental result as shown in Fig. 5-29.

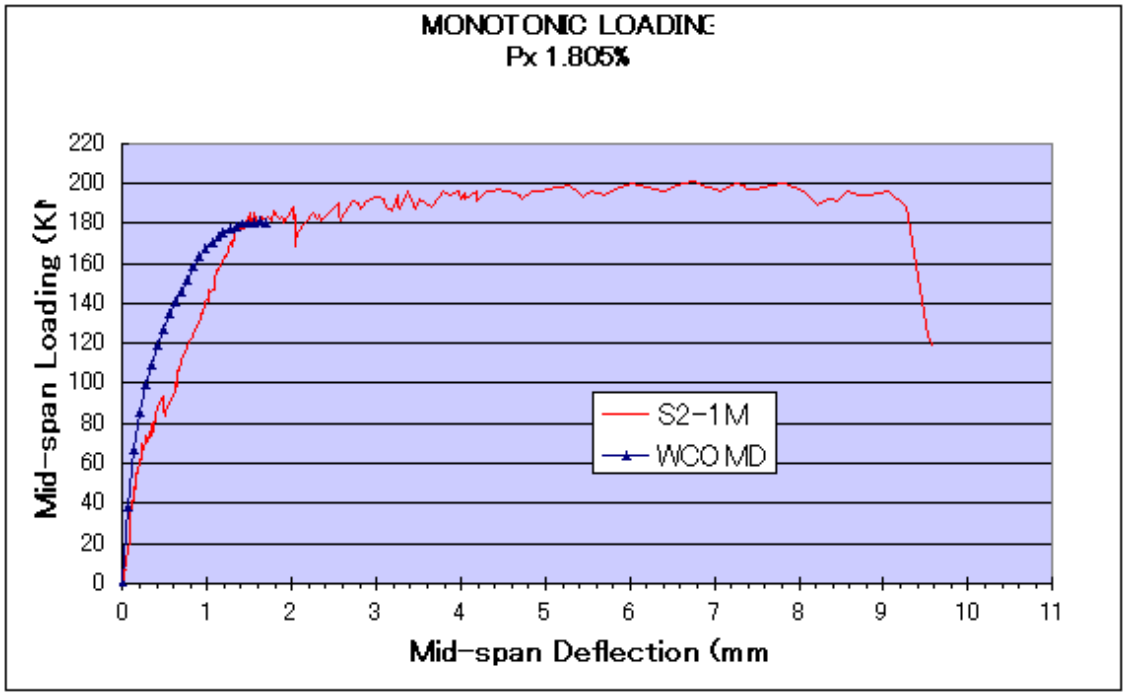

Fig. 5-29 Comparison of analytical and experimental results.

The crack pattern of analytical and experimental is shown in Fig. 5-30 and 5-31.

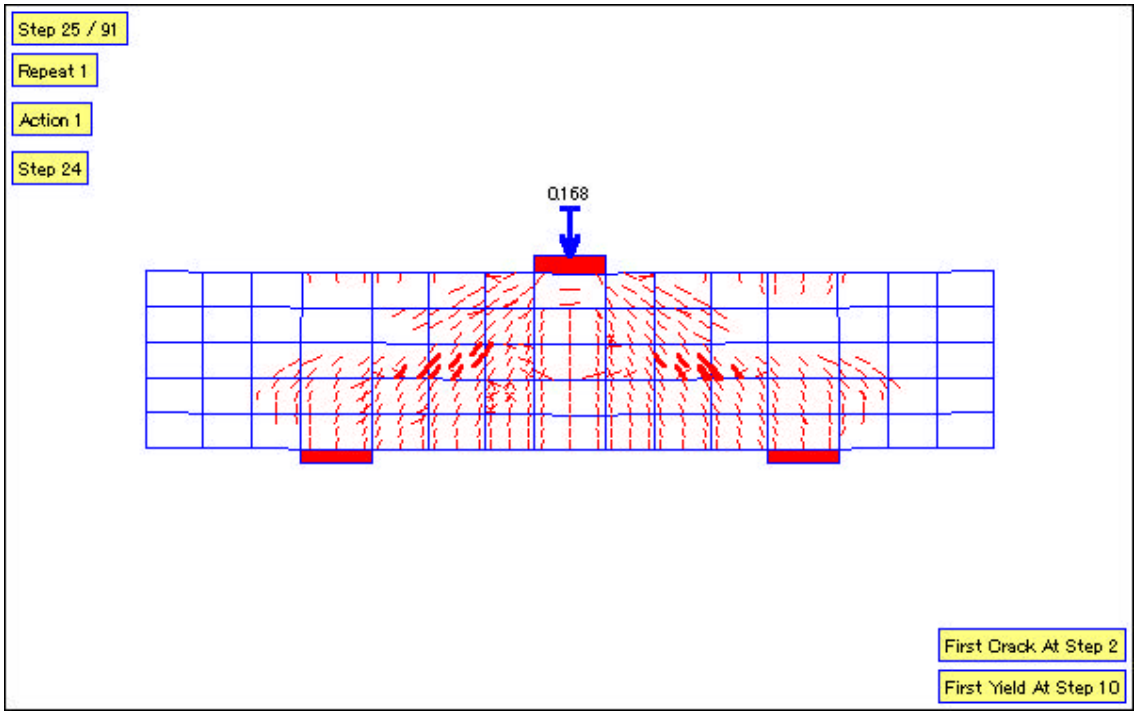

Fig. 5-30 Crack pattern of analytical result of specimen S2-1M

Fig. 5-31 Crack pattern of experimental result

The analytical result shows good agreement of yielding load with experimental one. After flexural crack is presented, deflection of experimental specimen will increase rapidly compare with analytical one. Strain hardening effect on experimental specimen is gradually increasing the load, while analytical model cannot govern this part. However for safe side, only accuracy of first yield load can cover design in real application in lower bound. Hence, the capability of present finite element program can cover the application of short beam with implementation of zoning method proposed by An. X. 1997.

CHAPTER 6

CONCLUDING REMARKS

6.1 Concluding Remarks

1. RC short beam without web reinforcement can sustain the shear force after forming of diagonal crack because of arch action, which transfers the load directly to support via diagonal compressive strut. Concrete strength in the web of RC beam is the main parameter to control crushing-shear failure mode.

2. Reversed loading will decrease ultimate deflection because of material deterioration, which results from crack opening and closing. Displacement ductility factor of the beam under reversed loading will reduce approximately by 40% of that one under monotonic loading.

6.2 Further Study

1. Shear strength of RC beam without web reinforcement is strongly related to compressive strength of concrete. Normal concrete with fc`30-35N/mm^2 is appropriate to compare with self-compacting concrete.

2. Application of deep beam with shear span to effective depth ratio 1.0-2.5 is widely used. Experimental extend should be cover this range.

3. To enhance the precision of experimental results, reversed loading couple with frame system should be implement.

4. To approach real application, RC with web reinforcement should be exist. Low reinforcement ratio is selected to study at first place.

REFERENCES

[1] James G. Macgregor, *Reinforced concrete-Mechanics and Design*, 3rd Ed., Prentice Hall,1997.

[2] Koichi Maekawa, Xuehui An, *Shear Failure and Ductility of RC Columns after Yielding of Main Reinforcement*, Journal of Engineering Fracture Mechanics 65 (2000) 335-368.

[3] An Xuehui, *Failure Aalysis and Evaluation of Seismic Performance for Reinforced Concrete in Shear*, Doctoral Doisertation, The University of Tokyo,1996, pp.25-28.

[4] R. Park and T. Paulay, *Reinforced Concrete Structures*, John Wiley & Sons, 1975 pp.549

[5] Hajime Okamura and Koichi Maekawa, *Nonlinear Analysis and Constitutive Model of Reinforced Concrete*, Tokyo, Japan, 1991

[6] Standard Specification For Design and Construction of Concrete Structures-1986, Part1 (Design), 1st Ed., JSCE

[7] Proceeding of The International Workshop on Self-Compacting Concrete, Concrete Engineering Series 30, JSCE, 1998

[8] Ouchi M., and Edamatsu Y., *A Rational Mix-Design for Mortar in Self-Compacting Concrete*, Proceeding of the Six East-Asia-Pacific Conference on Structural Engineering & Construction, Taipei, Taiwan, 1998

[9] Thomas T. C. Hsu, *Unified Approach to Shear Analysis and Design*, Journal of Cement and Concrete Composite 20 (1998) 419-435

[10] Paulus Irawan, *Three-Dimensional Analysis of Reinforced Concrete Structures*, Doctoral Dissertation, The University of Tokyo, 1995, pp.7-8, 130-139.